

1

1 **Gliding through marine heatwaves: Subsurface biogeochemical**
2 **characteristics on the Australian continental shelf**

3

4 Daneeja Mawren^{1,2,3*}, Julia Araujo⁴, Romain Le Gendre⁵, Jessica A. Benthuisen⁶, Franck Eitel
5 Kemgang Ghomsi^{1,7,8}, Jayanthi S. Saranya⁹, Amandine Schaeffer^{10,11}

6

7 ¹Department of Oceanography, University of Cape Town, Cape Town, South Africa

8 ²South African Environmental Observation Network, Egagasini Node, Roggebaai, South Africa

9 ³Mascarene Environmental Consulting, Ltd, Mauritius

10 ⁴National Center for Monitoring and Early Warning of Natural Disasters (CEMADEN), São José dos Campos, 12630-
11 000, Brazil

12 ⁵IFREMER, UMR 9220 ENTROPIE (IRD, Reunion Univ., IFREMER, New Caledonia Univ., CNRS), BP 32078,
13 98897 Noumea Cedex, New Caledonia

14 ⁶Australian Institute of Marine Science, Crawley, Western Australia 6009, Australia

15 ⁷Geodesy Research Laboratory, National Institute of Cartography, P.O. Box 157, Yaoundé, Cameroon

16 ⁸Centre for Earth Observation Science, University of Manitoba, Winnipeg, MB, Canada

17 ⁹School of Earth and Environmental Sciences, College of Natural Sciences, Seoul National University, Seoul,
18 Republic of Korea

19 ¹⁰School of Mathematics and Statistics, University of New South Wales, Sydney, New South Wales, Australia

20 ¹¹Centre for Marine Science and Innovation, University of New South Wales, Sydney, New South Wales, Australia

21 |

22 | * *Correspondence to:* Daneeja Mawren (daneejamawren@gmail.com)

23

24

25

3

4
26

Abstract

27 Marine heatwaves (MHWs) disrupt ecosystems across multiple trophic levels by altering oxygen and biological
28 productivity through the water column and yet, most studies focus on the surface, overlooking subsurface processes
29 that shape ecosystem responses. To address this gap, we analysed 16 years of routine and event-based glider
30 observations on the continental shelf around Australia to present the first comprehensive assessment of the subsurface
31 biogeochemical response during surface MHWs across four contrasting coastal regions.

32 Across all regions and seasons, the distribution of chlorophyll concentrations shifted towards a decline in the mixed
33 layer and an increase below the mixed layer during MHWs, modulated by the event categories. Dissolved oxygen
34 shows a more complex distribution, which also varies during moderate and strong MHW events, arguably with more
35 variation in the mixed layer than below.

36 When regional and seasonal specificities are taken into account, the subsurface characteristics of MHWs vary in
37 accordance with the environmental setting, including the continental shelf structures, tropical / sub-tropical regimes,
38 and boundary current influences, especially through the changes in stratification. Summer surface MHWs were
39 characterised by a shallower mixed layer depth than normal conditions and enhanced stratification, confining warming
40 to the upper ocean, while other seasons allow deeper penetration under weakly stratified conditions. With the shoaling
41 of the mixed layer, enhanced stratification retained nutrients within the euphotic zone, allowing phytoplankton to form
42 deeper and intensified chlorophyll maxima. The depth of maximum stratification therefore emerged as a useful proxy
43 for the vertical extent of MHWs.

44 ~~Marine heatwaves (MHWs) disrupt ecosystems across multiple trophic levels by altering oxygen and biological~~
45 ~~productivity through the water column. Yet, most studies focus on the surface, overlooking subsurface processes that~~
46 ~~shape ecosystem responses, particularly under compound events involving multiple co-occurring extreme~~
47 ~~environmental conditions. To address this gap, we analysed 16 years of routine and event-based glider observations~~
48 ~~on the continental shelf around Australia to present the first comprehensive assessment of the subsurface~~
49 ~~biogeochemical response during surface MHWs across four contrasting coastal regions. Summer surface MHWs were~~
50 ~~characterised by a shallower mixed layer depth than normal conditions and enhanced stratification, confining warming~~
51 ~~to the upper ocean, while other seasons allow deeper penetration under weakly stratified conditions. Stratification~~
52 ~~favoured deeper and intensified deep chlorophyll maxima, aligned with the depth of stratification maxima, and~~
53 ~~emerged as a useful proxy for the vertical extent of MHWs. Across all regions and seasons, for non-MHW conditions,~~
54 ~~dissolved oxygen had a bimodal distribution above and below the mixed layer. However, this distribution changed~~
55 ~~with event severity and included greater concentrations of low dissolved oxygen and reduced concentrations of high~~
56 ~~dissolved oxygen during strong events. Below the mixed layer, the bimodal distribution was less apparent and oxygen~~
57 ~~concentrations during strong events were more concentrated towards middle values. During moderate and strong~~
58 ~~MHWs, chlorophyll concentrations declined in the mixed layer, albeit this trend was not apparent below it. Regional~~
59 ~~responses were related to the environmental setting, including the continental shelf structure and boundary current~~
60 ~~influences, underseoring the importance of region-specific monitoring to understand how MHWs influence~~

5

6
7

8

9

61 ~~biogeochemistry, and furthermore, their ecological consequences on coastal waters. The interaction between physical~~
62 ~~processes, such as seasonal circulation and stratification, and biological feedback, including the presence of deep~~
63 ~~chlorophyll maxima and potential oxygen production, highlights the complex biogeochemical responses to MHWs.~~

64 The interaction between physical processes, such as seasonal circulation and stratification, and biological feedback,
65 including the presence of deep chlorophyll maxima and potential oxygen production, highlights the complex
66 biogeochemical responses to MHWs, and underscores the importance of region-specific dynamics and the need for
67 more consistent observation strategy, including biogeochemical processes.

68

69 **Keywords**

70 Marine heatwaves; subsurface layers; stratification; biogeochemistry; chlorophyll; dissolved oxygen; glider
71 observations; in situ measurements; coastal waters; continental shelf; Australia.

72

73 **Short summary**

74 Using sixteen years of ocean glider observations, we show that marine heatwaves are characterised by shallower
75 mixed layers and can alter subsurface biogeochemistry across Australia's continental shelf. While surface chlorophyll
76 generally declined, strong stratification and event severity promoted deeper, intensified chlorophyll maxima while
77 subsurface oxygen responses varied. These findings underscore the importance of region-specific dynamics in shaping
78 ecological responses to marine heatwaves.

79

80 **Short summary**

81 ~~Using sixteen years of ocean glider observations, we show that marine heatwaves shoal the mixed layer and alter~~
82 ~~subsurface biogeochemistry across Australia's continental shelf. While surface chlorophyll generally declined, strong~~
83 ~~stratification and event severity promoted deeper, intensified chlorophyll maxima while subsurface oxygen responses~~
84 ~~varied. These findings underscore the importance of region-specific dynamics in shaping ecological responses to~~
85 ~~marine heatwaves.~~

86 **1. Introduction**

87 As the Earth's climate continues to warm, the frequency and intensity of extreme events are increasing due to
88 anthropogenic forcing (Frölicher et al., 2018; Laufkötter et al., 2020) with profound consequences for both ecosystems
89 and human societies (Smith et al., 2021; 2023). Marine heatwaves (MHWs) are defined as ~~long-lasting,~~ extremely
90 warm ocean temperature anomalies and have become an increasing focus of research for their important impacts on
91 ecosystems. A key factor controlling MHW characteristics, including their vertical extent, intensity and persistence,
92 is upper-ocean stratification (Schaeffer and Roughan, 2017; Schaeffer et al., 2023; Zhang et al., 2023). Global
93 stratification has intensified over recent decades, leading to widespread mixed layer shoaling and altered thermocline

10

11

12

13

14

94 [structure \(Alexander et al., 2019; Li et al., 2020; Kwiatkowski et al., 2020; Amaya et al., 2021; Zhang et al., 2023\).](#)

95 [At regional and coastal scales, stratification is further shaped by local thermal, salinity and mechanical processes that](#)

96 [regulate the vertical mixing and influence the occurrence of MHWs \(Fordyce et al., 2019; Amaya et al., 2021; Gao et](#)

97 [al., 2020; Schaeffer et al., 2023\).](#) Recent studies have shown that subsurface signatures of MHWs can differ

98 substantially from surface observations. For instance, during the 2019 North Pacific MHW (“The Blob”), subsurface

99 warming persisted long after surface temperatures returned to normal, leading to prolonged ecological stress at depth

100 (Amaya et al., 2020). Similarly, along the east coast of Australia in New South Wales (~~NSW~~), subsurface MHWs have

101 been documented with minimal surface expression, highlighting the need for vertical profiling, [particularly in coastal](#)

102 [regions where strong stratification, complex circulation and shallow bathymetry can amplify subsurface temperature](#)

103 [anomalies to fully capture subsurface dynamics](#) (Schaeffer and Roughan, 2017; Schaeffer et al., 2023). [Strong](#)

104 [stratification can trap heat near the surface or isolate warm anomalies below the mixed layer, allowing subsurface](#)

105 [MHWs to persist at depth](#) ~~Investigating the subsurface dynamics of MHWs in coastal areas is critical for assessing~~

106 ~~ecological and socio-economic impacts.~~

107

108 [Investigating subsurface dynamics of MHWs in coastal areas is therefore critical for assessing ecological and socio-](#)

109 [economic impacts.](#) In coastal regions and over continental shelves, subsurface biogeochemical processes play a central

110 role in sustaining vital ecosystem services such as biodiversity, carbon sequestration and nutrient cycling, while

111 supporting economic activities such as fisheries and aquaculture (Walsh, 1991; Siefert and Plattner, 2004; Marre et

112 al., 2015). When combined with MHWs, biogeochemical extremes can trigger severe ecological disruption,

113 amplifying existing environmental stressors, such as nutrient limitation (Cavole et al., 2016; Le Grix et al., 2020),

114 acidification, and deoxygenation (Tassone et al., 2022), ultimately reducing productivity and threatening marine

115 ecosystem health.

116

117 Understanding how MHWs influence key biogeochemical variables, such as chlorophyll-a concentrations and oxygen

118 levels, is essential for predicting ecosystem responses. For instance, nutrient scarcity during MHWs can limit

119 phytoplankton growth, while warmer waters increase metabolic demands in marine species, further straining

120 ecosystems (Chen et al., 2023). Although surface chlorophyll-a often decreases during MHWs (Le Grix et al., 2020),

121 responses vary depending on factors such as [light](#) latitude and nutrient availability (Sen Gupta et al., 2020; Noh et al.,

122 2022). In regions where stratification limits nutrient upwelling, phytoplankton productivity may decrease, whereas, at

123 higher latitudes ([where light is a limiting factor](#)), stratification can enhance productivity by maintaining phytoplankton

124 in the sunlit surface layers (Kwiatkowski et al., 2020). On a global scale, MHWs have been found to promote the

125 development of deep chlorophyll maxima, based on 17 years of biogeochemical-Argo float data (Ma and Chen, 2025).

126 Reduced dissolved oxygen during MHWs represents another critical issue, particularly in shallow coastal areas.

127 Warmer water temperatures decrease oxygen solubility, potentially leading to hypoxic conditions that can severely

128 affect marine life (Meier et al., 2018; Safonova et al., 2024). MHWs intensify this mismatch between oxygen supply

129 and demand, as respiration rates increase in response to higher temperatures, further depleting oxygen levels (Tassone

15

16

17

18

19

130 et al., 2022). Combined effect of MHWs, reduced oxygen levels, and habitat compression can trigger mass mortality
131 events across multiple taxa, including fish, seagrasses, and marine mammals (Sampaio et al., 2021; Holbrook et al.,
132 2022), while altered prey distribution and increased metabolic demands can produce cascading effects throughout
133 marine food webs (Smith et al., 2023; Gomes et al., 2024).

134

135 While long-term satellite-derived records of sea surface temperature (SST) and surface chlorophyll-a have advanced
136 our understanding of MHWs globally, they require concurrent in water measurements to assess the extent of
137 subsurface temperature extremes and biogeochemical changes given the range of ecological impacts that can occur
138 through the water column (Smith et al., 2023). Traditional in situ methods such as moored temperature measurements,
139 conductivity-temperature-depth, and expendable bathythermograph casts can provide vertical profiles, but these
140 observations are often limited in spatial and temporal coverage (Oliver et al., 2021; Malan et al., 2025; Le Gendre et
141 al., 2025) and rarely include biogeochemical observations. In addition, coastal numerical models offer valuable
142 simulations of subsurface thermal structures, but they require large amounts of high-resolution data for validation or
143 assimilation, as they remain prone to uncertainties in poorly observed regions (Lachkar et al., 2019).

144

145 Ocean gliders offer a major advancement in subsurface monitoring, through high-resolution, autonomous, and
146 continuous measurements of water temperature, salinity, and biogeochemical properties, including dissolved oxygen
147 and chlorophyll fluorescence (Testor et al., 2019). Although glider deployments have limited temporal coverage for
148 detecting extremes, their ability to sample across depths and regions provides an unprecedented view in shelf and
149 boundary current environments (Testor et al., 2019). These measurements can be used to infer stratification and
150 phytoplankton dynamics, thus providing the means to measure simultaneously oceanographic variables, stratification,
151 phytoplankton, and oxygen dynamics at depth. Furthermore, event-based approaches, where gliders are deployed
152 specifically to sample MHWs, can provide real-time, dynamic insights into the subsurface evolution and intensity of
153 these events, delivering essential input to immediate ecosystem response strategies (Davies et al., 2021; Benthuisen
154 et al., 2025). Previous studies have made notable strides on better understanding the subsurface dynamics and
155 biogeochemical variability using gliders off the Australian coast (Pattiaratchi et al., 2011; Schaeffer et al., 2016a,b;
156 Chen et al., 2019; Chen et al., 2020; Ridgway and Ling, 2023). However, most of these works focused
157 regions off the Australian coast or were limited to specific events, typically ranging from weeks to months, rather than
158 continual monitoring. While these studies did not explicitly focus on MHWs, gliders have been demonstrated as a
159 useful platform to capture the vertical extent of extreme warming, such as during the 2016 austral summer MHW off
160 northeastern Australia (Benthuisen et al., 2018), highlighting the role of glider observations to inform MHW
161 studies:“short-term” observations.

162

163 To address this gap, our study leverages data from the Australian Integrated Marine Observing System (IMOS) gliders
164 which provide high-resolution subsurface observations along the Australian continental shelf since 2007 (Pattiaratchi

20

21

22

165 et al., 2017). By combining these repeated glider measurements with satellite-derived surface data, we aim to provide
 166 a seasonal and regional comparison across four distinct Australian shelf regions, highlighting broader patterns of
 167 subsurface MHW characteristics and their impacts on key biogeochemical variables. Specifically, we test the
 168 following hypotheses: (1) surface MHWs can lead to reduced chlorophyll concentrations and lower dissolved oxygen
 169 levels at the surface; (2) despite surface reductions, MHWs may promote deeper chlorophyll maxima and higher
 170 dissolved oxygen concentrations at depth, potentially via enhanced subsurface productivity; (3) the depth extent of
 171 surface MHWs varies with regions and seasons, and therefore establishing seasonal and regional baselines are
 172 important to interpret anomalies; and (4) the severity of MHW-induced stratification modulates biogeochemical
 173 variables (dissolved oxygen and chlorophyll).

175 The following sections outline our approach and findings: Sect. 2 describes the SST and glider datasets, statistical
 176 methods, and MHWs metrics. ~~Sect.~~ **Section** 3.1 describes the characteristics of surface MHWs in the study regions.
 177 Hypotheses (1) and (2) are examined in Sect. 3.2, which investigates how MHW severity influences chlorophyll and
 178 dissolved oxygen within and below the surface mixed layer. Hypothesis (3) is addressed in Sect. 3.3, where we explore
 179 regional and seasonal variations in the depth extent of MHWs, stratification and associated biogeochemical profiles.
 180 Hypothesis (4) is evaluated across Sects. 3.2 and 3.3, which together assess how MHWs modulates subsurface
 181 biogeochemical signatures in different regimes, based on their stratification, chlorophyll and oxygen regimes. Finally,
 182 Sect. 4 discusses these findings in the context of previous global and Australian studies, leading to the Conclusions in
 183 Sect. 5.

186 **2. Data and Methods**

187 **2.1 Satellite dataset and surface MHW detection**

188 Given the coastal scale of our study, we used the National Oceanic and Atmospheric Administration (NOAA)
 189 CoralTemp v3.1¹ Sea Surface Temperature (SST) product, which integrates three L4 satellite SST analysis products, to
 190 provide a global, daily, gap-free gridded, night-time SST field at 0.05° horizontal resolution since 1985 (Skirving et
 191 al., 2020). This dataset is used to track surface MHWs in near real-time² using the definition and criteria of Hobday
 192 et al., (2016), which detects temperature events exceeding a locally determined upper threshold of the 90th percentile
 193 relative to the long-term day-of-the-year climatology for a minimum of five consecutive days, with no gap of more
 194 than two days. The baseline climatological period was defined here as a 30-year period between 1985 and 2014,
 195 following recommendations of Hobday et al. (2016). The MHW detection and analysis were performed using the
 196 Python module available at <https://github.com/ecjoliver/marineHeatWaves>. We extracted the SST dataset over the

1 CoralTemp v3.1 product's website: <https://coralreefwatch.noaa.gov/product/5km/index.php>.

2 NOAA Coral Reef Watch marine heatwave website: https://coralreefwatch.noaa.gov/product/marine_heatwave/.

30

31

197 period from 1 January 1985 to 30 June 2025 and the following MHW metrics were analysed over our study period
198 from 2009 to mid-2025: the total number of events, the mean duration of the MHW events, and the mean severity of
199 the MHW (Eq. 1; following Sen Gupta et al., 2020).

200

201 2.2 Glider dataset

202 To assess the subsurface structure of MHWs, our study benefited from the Australian national glider data acquisition
203 strategy set up in 2007 by the Ocean Gliders facility under [IMOS \(the Australia's Integrated Marine Observing System](#)
204 [\(IMOS; Pattiaratchi et al., 2017\)](#). Subsequently, IMOS enabled the routine deployment of gliders on the continental
205 shelves around Australia for sustainable observations. This facility has been augmented by event-based sampling of
206 MHWs since December 2018 (Benthuisen et al., 2025), delivering subsurface measurements of oceanographic
207 parameters along with other near-real time platforms during events (e.g. Box 2 of Capotondi et al., 2024). Ocean
208 gliders are autonomous vehicles which alter their buoyancy to travel up and down the water column while sampling
209 seawater properties (Rudnick, 2016). We used data from IMOS using Teledyne Webb Research Slocum Electric
210 Gliders (G1, G2 and G3), equipped with Seabird-CTD, WETLabs BBFL2SLO 3 Eco Puck sensor measuring
211 chlorophyll fluorescence, colored dissolved organic matter (CDOM) and 660 nm backscatter, and an Aanderaa
212 Oxygen optode (Pattiaratchi et al., 2011; Chen et al., 2020). Missions typically last between three to five weeks, with
213 a maximum depth of 200 m. For this study, we focus on measurements of ocean temperature, salinity, chlorophyll-a
214 fluorescence (proxy for phytoplankton concentration; Blondeau-Patissier et al., 2014), and dissolved oxygen. The
215 measurements undertake a delayed-mode quality control (Woo and Gourcuff, 2023) and are made publicly available
216 through IMOS on the Australian Ocean Data Network (AODN) Portal³.

217

218 2.3 Study regions

219 The analysis of all available deployments led us to the definition of four main regions of interest encompassing the
220 highest density of gliders transects between 2009 and 2025: (i) northeastern Australia off Queensland (QLD), confined
221 within the limits of 144.7° E to 148.0° E and 13.3° S to 19.7° S; (ii) southeastern Australia off New South Wales
222 (NSW), from 149.7° E to 154.7° E and 28.5° S to 36.7° S; (iii) southwest Western Australia (SW WA), from 113.2°
223 E to 116.1° E and 29.1° S to 33.5° S; and (iv) the eastern coast of Tasmania (TAS), from 146.8° E to 149.5° E and
224 40.5° S to 44.6° S (Fig. 1). These regions encompass contrasting continental shelf systems influenced by distinct
225 physical processes, enabling us to assess how MHWs impact biogeochemical conditions under different dynamics.

3 Australian Ocean Data Network (AODN) website: <https://portal.aodn.org.au/>.

33

34

35

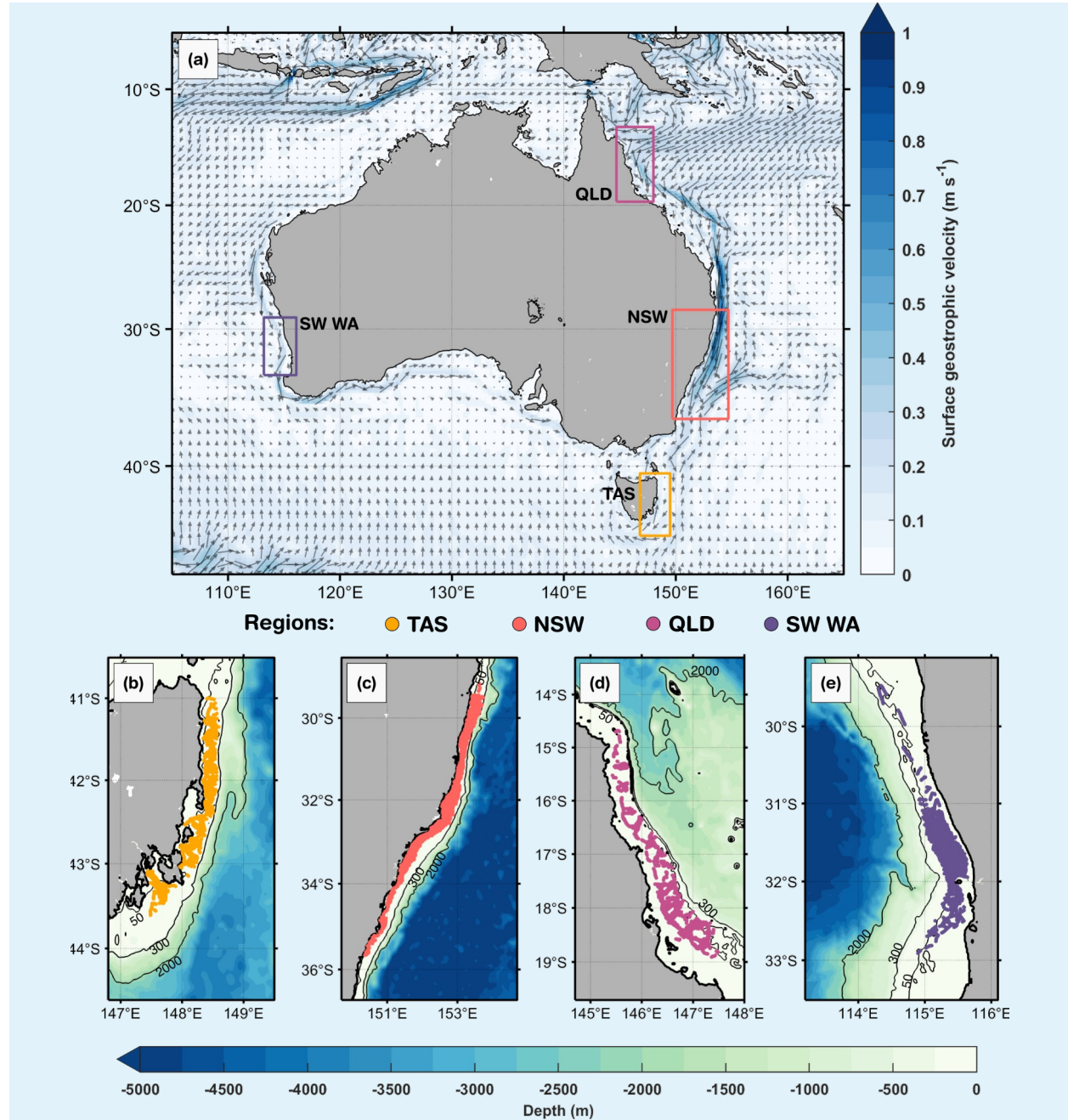


Figure 1. Study regions off the Australian coast. (a) Mean surface geostrophic currents (arrows) and highlighted boxes for each region of interest: northeastern Australia (Queensland region, QLD), southeastern Australia (New South Wales, NSW), southwest Western Australia (SW WA) and eastern Tasmania (TAS). Gliders' profile positions are illustrated in each sub-region: (b) TAS, (c) NSW, (d) QLD and (e) SW WA. In (a), the annual mean geostrophic currents were based on 1993 to 2020 and provided by the Integrated Marine Observing System (IMOS, <https://imos.aodn.org.au/oceancurrent>). Isobaths of 50 m, 300 m, and 2,000 m are shown in (b-e), derived from ETOPO1 bathymetry (Eakins & Sharman, 2010). Glider profiles are located over the continental shelf, in waters shallower than 200 m isobath..

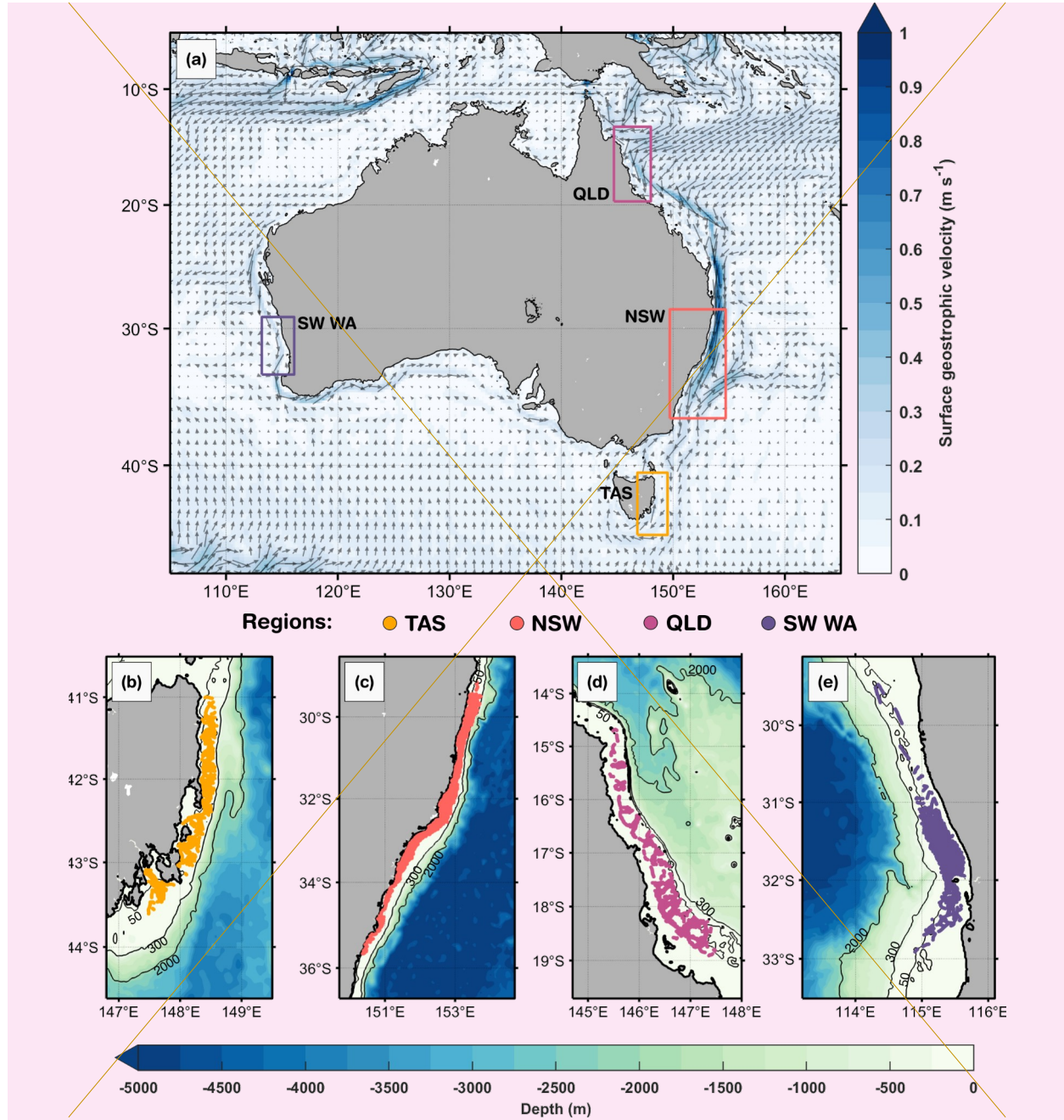


Figure 1. Study regions off the Australian coast. (a) Mean surface geostrophic currents (arrows) and highlighted boxes for each region of interest: northeastern Australia (Queensland region, QLD), southeastern Australia (New South Wales, NSW), southwest Western Australia (SW-WA) and eastern Tasmania (TAS). Gliders' profile positions are illustrated in each zoomed region: (b) TAS, (c) NSW, (d) QLD and (e) SW WA. In (a), the annual mean geostrophic currents were based on 1993 to 2020 and provided by the Integrated Marine Observing System (IMOS, <https://imos.aodn.org.au/oceancurrent>). Isobaths of 50 m, 300 m, and 2,000 m are shown in (b-e), derived from ETOPO1 bathymetry (Eakins & Sharman, 2010).

48

49

227 2.4 Profile selection and data processing

228 Glider deployments were selected to keep only those profiles within the aforementioned study regions, spanning a 16-
229 year period from January 2009 to June 2025. To ensure the quality of our analyses, the following quality control steps
230 were taken for each glider mission: (i) selection of only ‘good data’ flags (Woo & Gourcuff, 2023)⁴; (ii) removal of
231 chlorophyll outliers; (iii) applying a step to address non-photochemical quenching in chlorophyll observations; and
232 (iv) removal of data points inside the bottom boundary layer (BBL). To remove the noise from the chlorophyll
233 measurements (step (ii)), the outliers were identified based on a moving average of window size equivalent to 1,000
234 points along the glider sampling, discarding values above two standard deviations of the logarithmic chlorophyll.
235 Moreover, light-induced fluorescence leads to errors in sensor measurements of phytoplankton concentration
236 (quenching), causing high variability in chlorophyll-a fluorescence profiles. To mediate this effect (step (iii)), we used
237 only night-time data points, defined as any time before sunrise or after sunset (as in Schaeffer et al., 2016b). Regarding
238 the variable BBL contamination due to sloping topography, we removed data within 20 m above the seabed, similar
239 to Schaeffer et al. (2014, 2017). This threshold aims to minimize contamination from interference in the near-bottom
240 levels when aggregating the shelf profiles over various topographic depths for a combined analysis.

241

242 This study is focused on continental shelf watersshelves, and hence the fewrare measurements from deeper regions
243 were excluded. The continental shelf width and depth at the shelf-edge varies over each region. Off QLD and SW
244 WA, only measurements over bathymetry between 40 and 80 m were retained. For regions with deeper and steeper
245 continental shelves, i.e. TAS and NSW, - we retained measurements between 50 and 120 m. Finally, we separated the
246 data points into downward and upward casts, binned each cast into a 1 m vertical resolution, averaged each pair of
247 down/upward casts, and binned the averaged profiles into fixed distances of 1 km horizontal resolution, which is more
248 than the median distance between profiles (e.g. 100–200 m in NSW region, Schaeffer et al., 2016b). These last steps
249 enable vertical and horizontal consistency of profiles, avoid glider’s direction bias when averaging the down/upward
250 casts, and reduce noise for shelf-scale comparison of subsurface MHW signals. In Fig. S1, we illustrate a glider
251 mission before and after quality control steps mentioned above.

252

253

254 2.5 Classifying MHW vs non-MHW profiles

255 We classify MHW and non-MHW glider profiles by first collocating MHW severity index in time and space using the
256 satellite SST dataset. Thus, the severity index (S) was calculated for each profile following Sen Gupta et al. (2020),
257 as below:

4

https://content.aodn.org.au/Documents/IMOS/Facilities/Ocean_glider/Delayed_Mode_QAQC_Best_Practice_Manual_OceanGliders_LATEST.pdf

50

51

52

53

54

$$S_{i,d} = \frac{SST_{i,d} - SST_{i,d}^{clim}}{SST_{i,d}^{PC90} - SST_{i,d}^{clim}} \quad (1)$$

259 where $SST_{i,d}^{clim}$ is the long-term daily mean SST on the d th day of the year at location i , $SST_{i,d}^{PC90}$ is the 90th percentile
 260 of SST on the same day and location as the glider profile. The MHWs were ~~classified~~ categorized into four types: (i)
 261 moderate, $1 < S \leq 2$; (ii) strong, $2 < S \leq 3$; (iii) severe, $3 < S \leq 4$, and (iv) extreme ($S > 4$) following the category
 262 indices proposed in Hobday et al. (2018). For each study region, the mean location of the glider profiles was
 263 determined, and time series of the severity index were derived, enabling the representation of an ‘average’ severity
 264 timeline for each region (see Figs. 1b-e).

265

~~Then, using glider data, the seasonal climatology at each depth was computed for each region by averaging profiles
 266 over 3-month periods (austral summer – December/January/February, autumn – March/April/May, winter –
 267 June/July/August, and spring – September/October/November). Note that the profiles showing negative seasonal
 268 anomalies *in situ* surface temperature were excluded from the satellite-based MHW classification. These discrepancies
 269 may arise due to different datasets used, methodology when computing anomalies and also due to the sampling
 270 locations of these profiles. For instance, given the wide area selected for New South Wales, the southern part of the
 271 region is cooler than the northern region. As a result, in comparison to the mean profile, the southern profiles may
 272 potentially present a cool anomaly.~~

274

275 2.6 In situ subsurface parameters

276 To further ~~characterise~~ characterize the surface-MHWs in subsurface layers, some proxies were ~~used~~ defined, such as:
 277 (i) ~~mixed layer depth (MLD)~~; (ii) ~~thermocline depth~~; (iii) ~~buoyancy frequency, i.e. degree of stratification~~; (iv)
 278 ~~dissolved oxygen saturation~~; (v) ~~MHW depth extent, defined as depth containing 90% of the vertical heat content~~
 279 ~~anomaly~~; (vi) ~~MHW depth extent, as the depth of positive temperature anomalies based on the seasonal regional mean~~
 280 ~~temperature profile~~; (ii) ~~mixed layer depth (MLD)~~; (iii) ~~thermocline depth~~; (iv) depth of maximum stratification,
 281 defined as the depth at which the buoyancy frequency reaches its maximum value in the water column; ~~and (vii)~~
 282 ~~depth of deep chlorophyll maxima (DCM). For anomaly calculations in the subsurface, we use non-MHW profiles as~~
 283 ~~our baseline, i.e. anomalies are calculated relative to the mean non-MHW profile. This provides a physically consistent~~
 284 ~~background state and avoids potential bias introduced by uneven sampling of MHW and non-MHW profiles.~~
 285 ~~Therefore, we define the seasonal mean composite for each region as the average non-MHW profiles over 3-month~~
 286 ~~seasonal periods (austral summer - December/January/February, autumn - March/April/May, winter -~~
 287 ~~June/July/August, and spring - September/October/November); and (vi) dissolved oxygen saturation.~~

288

289 The MLD was computed for each individual temperature profile by identifying the shallowest depth at which the
 290 absolute temperature difference from the surface (0 m) exceeded a fixed threshold of 0.2° C. This threshold-based

55

56

57

291 method is commonly applied to in situ observations due to its physical relevance in stratified ocean conditions (e.g.,
 292 de Boyer Montégut et al., 2004). Profiles with missing surface data or insufficient vertical resolution near the surface
 293 were excluded from MLD calculations. MLD estimates were then averaged seasonally and grouped into MHW and
 294 non-MHW categories, based on the presence or absence of MHW conditions.

296 The thermocline depth was computed from the vertical temperature profiles by calculating the temperature gradient
 297 with respect to depth. The depth corresponding to the maximum negative gradient (i.e. the strongest rate of temperature
 298 decrease with depth) was defined as the thermocline depth.

300 The buoyancy frequency, also called the Brunt Väisälä frequency, represents the degree of stratification and is defined
 301 as:

$$N^2 = -\frac{g}{\rho_0} \frac{\partial \rho}{\partial z}$$

(2)

304 where ρ_0 represents the background density, g is the gravitational constant and $\frac{\partial \rho}{\partial z}$ denotes the vertical gradient
 305 of potential density. The density was calculated from the glider's vertical temperature and salinity profiles.

307 Dissolved oxygen saturation was computed from temperature, salinity and pressure following standard solubility
 308 formulations, using the García and Gordon (1992) equation for seawater. Hence, oxygen saturation was calculated as
 309 the ratio between measured dissolved oxygen concentration and the corresponding solubility value at in-situ
 310 conditions. This provides a temperature- and salinity-adjusted measure of oxygen availability relative to atmospheric
 311 equilibrium, making it a useful indicator of both biogeochemical processes (production and respiration) and physical
 312 transport mechanisms (vertical mixing and horizontal advection) that influence oxygen independently of solubility
 313 changes.

315 MHW depth extent is defined as the depth which contains 90% of the vertical heat content anomaly, following
 316 Elzahaby and Schaeffer (2019). For each MHW profile, positive temperature anomalies ($\Delta T > 0$) are integrated
 317 vertically, and the depth extent corresponds to 90% of the profile's cumulative temperature anomaly. This approach
 318 provides a physically consistent estimate of the vertical penetration of the MHW-associated warming relative to
 319 background (non-MHW) conditions.

321 ~~To evaluate the relationships between physical and biogeochemical variables during MHWs, we calculated the~~
 322 ~~correlations by regions and seasons separately. The variables considered include MHW depth extent, depth of~~
 323 ~~maximum stratification, deep chlorophyll maximum (DCM) depth, thermocline depth, dissolved oxygen (DOX)~~
 324 ~~anomalies, chlorophyll (CPHL) anomalies, and temperature anomalies above and below the MLD. Several restrictions~~
 325 ~~were applied to ensure that the correlations were unbiased.~~

63

64

325 | (a) All MHW profiles were included to increase the number of data points and improve statistical robustness.

326 | (b) Depths shallower than 5 m and within 5 m of the bottom (based on the maximum depth after QC), were
327 | excluded for all depth-related metrics (thermocline depth, MHW depth extent, DCM depth, and depth of
328 | stratification maximum) to avoid surface and near-bottom artefacts.

329 | (c) Only stratified profiles were retained following the following methodology:

330 | (i) Identify the depth of maximum stratification,

331 | (ii) Calculate the seasonal 25th percentile of stratification,

332 | (iii) Profiles exceeding this threshold were classified as stratified.

333 | This approach excludes winter or homogeneous profiles that would otherwise give false strong correlations.

334 | (d) Correlations were considered significant only if the p-value was less than 0.005 and the number of data
335 | points was greater than 30.

336 | (e) The MHW depth was calculated as follows:

337 | (i) Identify the last positive temperature anomaly from the surface before it turns negative,

338 | (j) Discard profiles where the entire temperature anomaly profile was entirely negative or
339 | positive (i.e. discard well-mixed profiles).

340

341 | To evaluate the relationships between physical and biogeochemical variables during MHWs, we calculated the
342 | correlations by regions and seasons separately. The variables considered include MHW depth extent, depth of
343 | maximum stratification, depth of DCM, thermocline depth, dissolved oxygen (DO) anomalies, chlorophyll (CHL)
344 | anomalies, and temperature anomalies above and below the MLD. Several restrictions were applied to ensure that the
345 | correlations were unbiased.

346 | (a) Only stratified profiles were retained, when the profile maximum buoyancy frequency (N^2) exceeded the
347 | 75th percentile of the regional distribution of maximum N^2 values. This approach excludes homogeneous
348 | and weakly stratified profiles, often present in winter, that would otherwise give false strong correlations.

349 | (b) Profiles lacking any positive subsurface temperature anomalies, since some of these metrics are undefined in
350 | these cases and their inclusion would bias correlations toward spurious zero-inflation.

351 | (c) Depths shallower than 5 m and within 5 m from the bottom were excluded to avoid surface and near-bottom
352 | artefacts.

353 | (d) Correlations were considered significant only if the p-value was less than 0.05 and the number of data points
354 | was greater than 30 (Fig. S8).

355

356 | 2.7 Summary of glider missions in surface MHWs

357 | Across the four study regions, a total of 202 glider missions were recorded over the continental shelf between January
358 | 2009 and June 2025, with the highest number off SW WA (77 glider missions) and NSW (56 missions), followed by
359 | TAS (41 missions) and QLD (27 missions). These missions yielded 61,280 profiles (Table 1), with NSW and SW WA

65

66

67

360 contributing the largest to the dataset (19,785 and 19,355 profiles, respectively), and fewer profiles in TAS (11,699)
 361 and QLD (10,441). These glider missions and their associated profiles were distributed seasonally, with and without
 362 MHW encounters (Table 1, Figs. 2b, d, f, h). Note that the number of chlorophyll profiles is lower than for other
 363 variables because of (i) quality control steps, (ii) removal of chlorophyll outliers and (iii) fluorescence quenching as
 364 described in sect. 2.4, and these data are presented in Supplementary Table S1.

366 **Table 1. Seasonal number of profiles with and without MHWs by region, as northeastern Australia (Queensland region,**
 367 **QLD), southwest Western Australia (SW WA), southeastern Australia (New South Wales, NSW) and eastern Tasmania**
 368 **(TAS).**

		<u>Number of profiles</u>				
		<u>Summer (DJF)</u>	<u>Autumn (MAM)</u>	<u>Winter (JJA)</u>	<u>Spring (SON)</u>	<u>Total profiles</u>
TAS	<u>MHW</u>	<u>499</u>	<u>1,007</u>	<u>31</u>	<u>150</u>	11,699
	<u>Non MHW</u>	<u>1,450</u>	<u>2,535</u>	<u>2,181</u>	<u>3,846</u>	
	Total	1,949	3,542	2,212	3,996	
NSW	<u>MHW</u>	<u>294</u>	<u>989</u>	<u>342</u>	<u>1,167</u>	19,785
	<u>Non MHW</u>	<u>2,019</u>	<u>3,283</u>	<u>4,675</u>	<u>7,016</u>	
	Total	2,313	4,272	5,017	8,183	
QLD	<u>MHW</u>	<u>788</u>	<u>2,269</u>	<u>894</u>	<u>619</u>	10,441
	<u>Non MHW</u>	<u>1,697</u>	<u>953</u>	<u>1,300</u>	<u>1,921</u>	
	Total	2,485	3,222	2,194	2,540	
SW WA	<u>MHW</u>	<u>953</u>	<u>512</u>	<u>187</u>	<u>139</u>	19,355
	<u>Non MHW</u>	<u>3,751</u>	<u>4,251</u>	<u>5,611</u>	<u>3,951</u>	
	Total	4,704	4,763	5,798	4,090	
		<u>Number of profiles</u>				
		<u>Summer (DJF)</u>	<u>Autumn (MAM)</u>	<u>Winter (JJA)</u>	<u>Spring (SON)</u>	<u>Total profiles</u>
QLD	<u>MHW</u>	<u>788</u>	<u>2,269</u>	<u>894</u>	<u>619</u>	10,441
	<u>Non MHW</u>	<u>1,697</u>	<u>953</u>	<u>1,300</u>	<u>1,921</u>	
	Total	2,485	3,222	2,194	2,540	
SW WA	<u>MHW</u>	<u>953</u>	<u>512</u>	<u>187</u>	<u>139</u>	19,355
	<u>Non MHW</u>	<u>3,751</u>	<u>4,251</u>	<u>5,611</u>	<u>3,951</u>	

	Total	4,704	4,763	5,798	4,090	
NSW	MHW	294	989	342	1,167	19,785
	Non-MHW	2,019	3,283	4,675	7,016	
	Total	2,313	4,272	5,017	8,183	
TAS	MHW	499	1,007	31	150	11,699
	Non-MHW	1,450	2,535	2,181	3,846	
	Total	1,949	3,542	2,212	3,996	

369

370 NSW recorded the greatest number of MHW missions, with 12 separate glider deployments encountering MHW
371 conditions in spring and 10 in autumn (Fig. 2d), corresponding to 1,167 and 989 MHW profiles, respectively (Table
372 1). In SW WA, most missions and profiles occurred in winter and autumn, yet MHW missions (profiles) were more
373 frequent in summer (10 MHW gliders; 953 MHW profiles) and autumn (7 MHW gliders; 512 MHW profiles) (Fig.
374 2h, Table 1). TAS also recorded the highest number of MHW profiles in autumn (1,007 profiles, over 7 missions) and
375 summer (499 profiles, over 5 missions) (Fig. 2b, Table 1). In contrast, QLD showed missions with a more even
376 seasonal spread (Fig. 2f; Table 1), with MHW gliders and profiles more common in winter (5 missions; 894 profiles)
377 and autumn (5 missions; 2,269 profiles), this last season being the greatest number of MHW profiles among all seasons
378 and regions. Despite an overall lower number of MHW missions in QLD, the proportion of MHW profiles relative to
379 the total profiles was higher compared to other regions (Figs. 2e, g, Table 1). This reflects the fact that MHWs in QLD
380 are longer-lasting (Fig. 3h), and therefore glider deployments are more likely to capture them.

381

382 The vertical distribution of glider profiles also varied across regions due to distinct sloping topography (Figs. 2a, c, e,
383 g), with the highest profile density extending to depths of up to 100 m off TAS and NSW, while profiles were
384 generally shallower (mostly less than 60 m) off QLD and SW WA. MHW profiles, although consistently fewer than
385 non-MHW profiles, were more frequent in the upper 20 m (Figs. 2a, c, e, g) than at the surface or at deeper layers. To
386 ensure a robust representation of the vertical structure, profiles were truncated at depths where less than 10% of
387 profiles were available (and 20% for QLD and SW WA), resulting in a maximum analysed depth of 90 m for NSW
388 and TAS, 40 m for QLD, and 30 m for SW WA.

389

390 The severity of MHW profiles further highlighted regional differences (Fig. 2i). Most events were classified as
391 Category 1 (“Moderate”), with the highest numbers recorded in QLD (3660 profiles) and NSW (2472 profiles).
392 Category 2 (“Strong”) MHWs were most frequently sampled off QLD with 910 profiles, followed by 320 profiles off
393 NSW, 203 profiles off TAS, and 134 profiles off SW WA. Category 3 (“Severe”) events were fewrare and only
394 sampled off TAS (11 profiles), while Category 4 (“Extreme”) events were not sampled over the continental shelf after

78

79

395 quality control steps. Together, these patterns reflect regional contrasts in the number of glider missions, the seasonal
396 and vertical distribution of profiles, and the severity of MHW conditions observed.

397 |

398 |

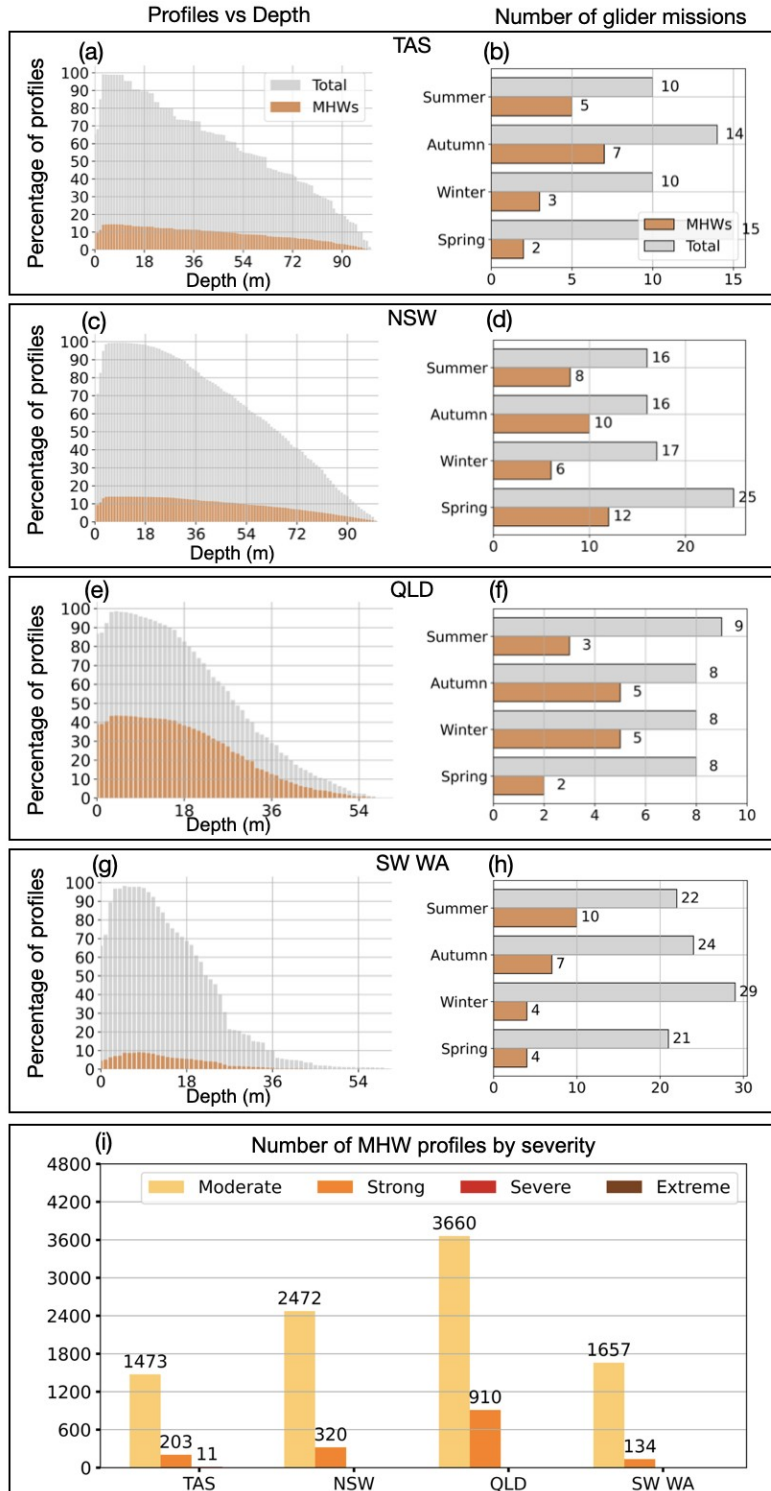
399

400

80

81

82



401

402

403

404

405

406

Figure 2. (a,c,e,g) Depth distribution of profiles for Tasmania (TAS), New South Wales (NSW), Queensland (QLD) and southwest Western Australia (SW WA), showing the percentage of total profiles (grey) and MHW profiles (orange) at each depth. (b,d,f,h) Seasonal counts of glider missions for each region, with total missions in grey and MHW missions in orange. (i) Number of MHW profiles per region, classified by severity: moderate, strong, severe and extreme. A glider is classified

88

89

407 as being in a MHW based on its position and whether a surface MHW was identified there from the NOAA CoralTemp
408 v3.1 SST with a reference period of 1985-2014.

409

410 3. Results

411 3.1 Characteristics of surface marine heatwaves

412 Regional variations in surface MHW metrics derived from satellite SST are illustrated in Fig. 3. From 2009 to
413 mid-2025, the eastern ~~TAS region Tasmanian coast (TAS)~~ experienced over 80 surface MHWs (Fig. 3a), whereas
414 fewer than 40 events were detected along the continental shelf. Around Storm Bay in southeast TAS (43° S, 147.5°
415 E), where most gliders were initially deployed, MHWs were generally long-lasting with mean durations of 27-31 days
416 and mean severity exceeding 1.80 (Figs. ~~3e, i3b, e~~). To better capture the temporal distribution of MHWs relative to
417 glider sampling, a timeline analysis was performed for each region (Fig. 4). MHWs in the TAS region were most
418 frequent from November through to April, with strong to severe events concentrated between January and February
419 (Fig. 4a). In several instances, glider profiles sampled prolonged, strong to severe (Fig. 2i) MHWs, with severity
420 indices exceeding 3, including April 2016, February 2019, January 2022, and December 2023 (Fig. 4a).

421

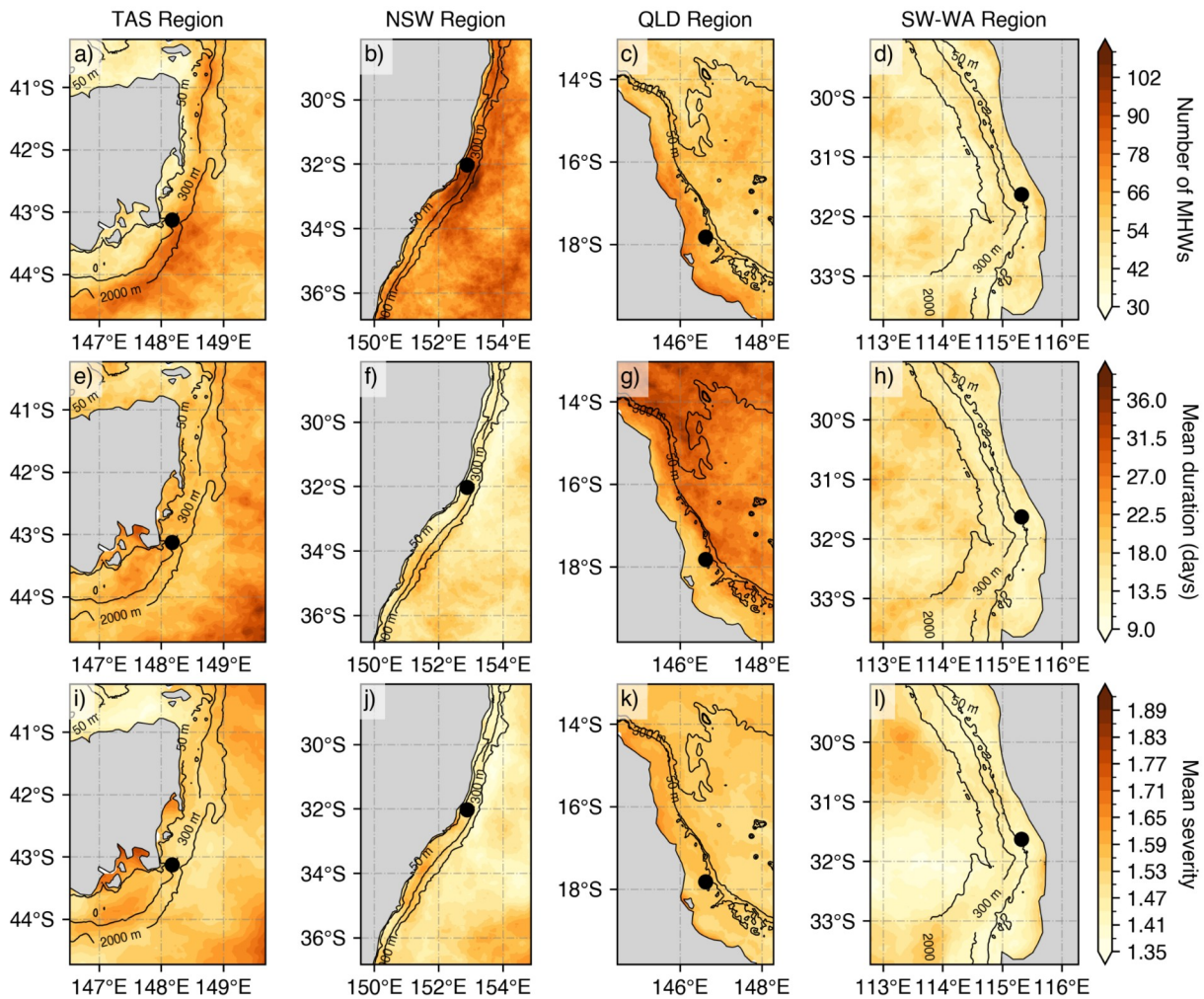
422 Relative to other Australian regions, NSW exhibited the highest occurrence of MHWs, with more than 100 MHWs
423 detected over the study period (Fig. ~~3b3d~~). This highly dynamic region is typically characterised by short-lived MHWs
424 lasting less than 10 days (Fig. ~~3f3e~~). On the ~~continental inner~~ shelf, the mean severity of MHWs in NSW did not exceed
425 1.65, which is lower than that observed off TAS. However, two short-lived but severe events in September 2013, and
426 October 2018 (Fig. ~~4b4e~~), exceeded a severity index of 3. Glider missions deployed during these periods sampled
427 through the tail of the events, capturing a maximum severity value of 2.1 and 1.6, respectively.

428

90

91

92



429

430 **Figure 3. Mean surface MHW metrics based on NOAA CoralTemp v3.1 (climatology 1985-2014 reference period) over the**
 431 **gliders' deployment period (1 January 2009 - 30 June 2025) by regions: (a-e-i) eastern Tasmania (TAS), (b-f-j) southeastern**
 432 **Australia (New South Wales, NSW), (c-g-k) Queensland region (QLD), and (d-h-l) southwest Western Australia (SW WA).**
 433 **The top panels represent the number of MHWs, the middle panels show the mean duration (in days), and bottom panels**
 434 **indicate the mean MHW severity. MHW severity values are calculated from selected SST pixels (black point) representative**
 435 **of the glider study regions off TAS (148.175° E, 43.125° S), NSW (152.575° E, 32.025° S), QLD (146.625° E, 17.825° S) and**
 436 **SW WA (115.325° E, 31.625° S).**

437

438

439 Off northeast Australia (north of 20°S), MHWs were more frequent over the continental shelf, with 66-78 occurrences
 440 recorded, compared to fewer events in offshore waters (waters deeper than 200-300 m isobaths Fig. 3c), Fig. 3g). In
 441 agreement with the higher frequency, MHWs on the continental shelf were shorter in duration (Fig. 3g), whereas
 442 while offshore events were generally more prolonged, lasting 28–36 days on average. Across the central to northern
 443 Great Barrier Reef (GBR)GBR off QLD, the severity of MHWs typically had mean values below 1.65. However,

95

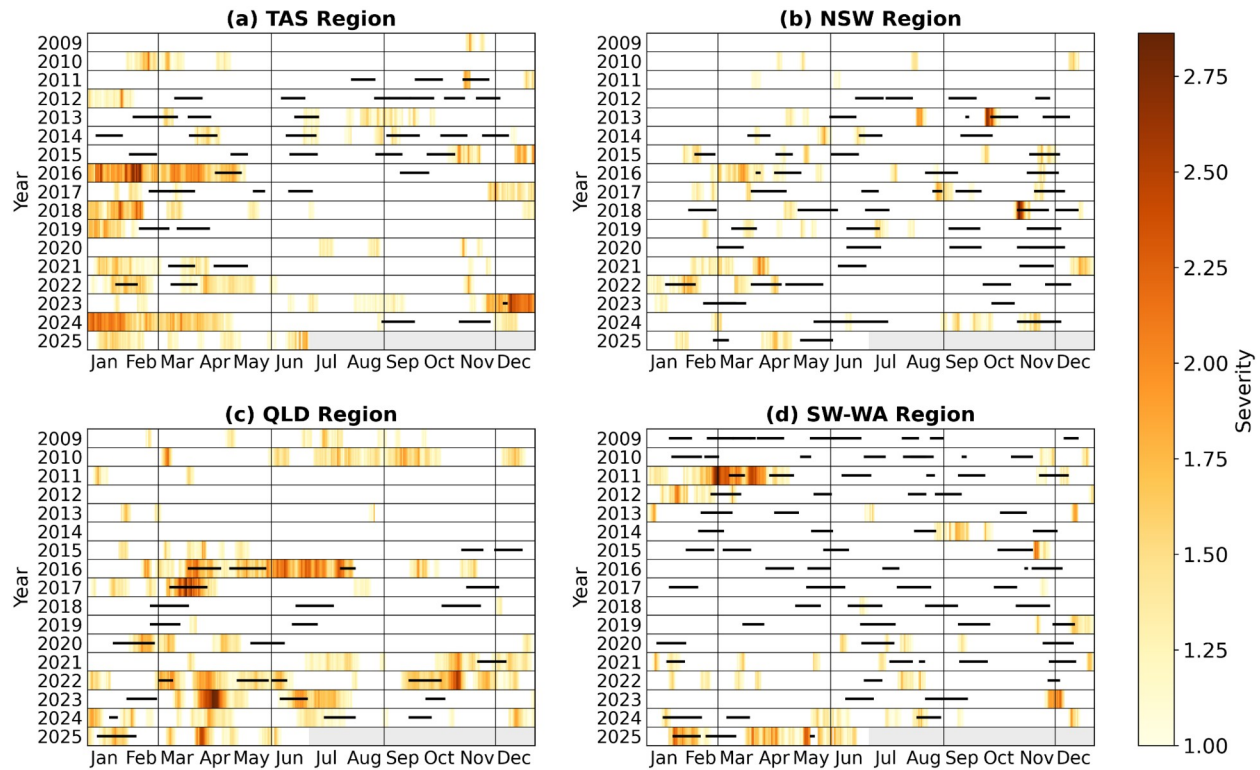
444 there have been events with longer duration and higher severity over the continental shelf, particularly between autumn
445 and winter, in the past decade (Fig. 4c4d). These intense seasonal events also coincided with a higher proportion of
446 MHW gliders during these seasons (Fig. 2g). The 2016 MHW stood out as a prolonged (more than 5 months) and
447 severe event captured by three glider missions that sampled the onset (maximum severity: 2.6), middle (maximum
448 severity: 2.3) and tail (maximum severity: 2.6) of the event. Additional severe MHWs were also sampled in March
449 2017 (maximum severity: 2.9) and September 2022 (maximum severity: 2.1). It is important to note that while some
450 deployments shown in Fig. 4 coincided with severe satellite-detected MHWs, several profiles were excluded during
451 quality control, and therefore may not fully reflect peak severity of the event.

453 In contrast to eastern Australia, MHWs off the SW WA were shorter (less than 10 days on average; Fig. 3k), less
454 frequent with less than 45 MHWs recorded (Fig. 3j) and generally weaker in severity ranging between 1.3-1.5 (Fig.
455 3l). The low severity of MHWs in SW WA appears to be influenced by periods of sustained MHW cold spells off the
456 west coast, which contributed to the lower mean values over the study period (Feng et al., 2021). Such prolonged and
457 cold events can dampen the long-term mean MHW metrics, while other regions in eastern Australia experience a
458 higher prevalence of MHWs with greater duration and intensity. As indicated by the number of glider missions and
459 MHW profiles (Fig. 2h and Table 1), events in SW WA were more frequent and severe between summer and autumn
460 (Fig. 4d). While routine missions are conducted throughout the year, targeted MHW deployments are more likely to
461 occur during summer and autumn, when ocean temperatures are highest and MHW risk is elevated. Increased 4b).
462 These seasonal peaks coincided with increased glider sampling efforts may contribute to increased in situ observations
463 of MHWs during these seasons, although the seasonal peak in MHWs is also evident in the satellite record (Fig. 4d),
464 indicating that the pattern is not only due to sampling effort that complemented satellite observations. The prolonged
465 2011 MHW is a key event in the region marked by strong to extreme severity nearshore. This event was sampled by
466 two glider missions, one in March (maximum severity: 2.1) and the other in April (maximum severity: 1.6). More
467 recently, in early 2025, SW WA experienced another prolonged, moderate to strong MHW in the region which was
468 also sampled by two glider missions at two critical stages: during the peak (maximum severity: 2.2) and decline
469 (maximum severity: 1.4) of the event, capturing the different phases of the event.

471 These glider observations were critical, not only in validating satellite-derived MHW metrics across regions and
472 seasons, but also in offering detailed subsurface insights beyond satellite capabilities.

103

104



475

476

477

478

479

480

481

482

Figure 4. Occurrence and severity of MHWs from January 2009 to June 2025 for (a) Tasmania (TAS), (b) New South Wales (NSW), (c) Queensland (QLD), and (d) southwest Western Australia (SW-WA), with horizontal black lines indicating periods when glider missions occurred. Light gray bars in 2025 indicate times beyond the study period. Vertical grey lines delineate seasons. MHW severity values are calculated from selected SST pixels representative of the glider study regions off TAS (148.175° E, 43.125° S), SW-WA (115.325° E, 31.625° S), NSW (152.575° E, 32.025° S), and QLD (146.625° E, 17.825° S).

483

3.2 Marine heatwave severity influences on chlorophyll concentrations and dissolved oxygen

484

485

486

487

488

489

490

491

492

This section examines the impact of surface MHW severity on both surface and subsurface changes in chlorophyll concentrations and DO dissolved oxygen (DOX)-levels from glider-sampled MHWs over the Australian continental shelf. Fig. 5 compares chlorophyll and DOX distributions between non-MHW periods and MHW categories (moderate and strong), above and below the MLD mixed layer depth (MLD), combining data across all regions. Above the MLD, non-MHWs display a broader chlorophyll fluorescence distribution compared to MHWs, whereas below the MLD, the probability distributions show minimal variations. DOX, on the other hand, shows distinct shifts in probability densities under MHW conditions, with multimodal peaks apparent both within and below the MLD in both layers, reflecting underlying regional and seasonal variations.

105

106

107

109
493 Within the mixed layer, chlorophyll concentrations generally decrease during MHWs (Fig. 5a; thick curves) compared
494 to non-MHW conditions. Non-MHW conditions show a peak around 0.7 mg m^{-3} , whereas moderate MHWs peak near
495 0.25 mg m^{-3} , and strong MHWs around 0.23 mg m^{-3} , indicating progressively stronger decrease of chlorophyll
496 concentrations in the MLD under increasing MHW severity. Below the MLD, non-MHW conditions show lower
497 subsurface chlorophyll ($\sim 0.25 \text{ mg m}^{-3}$) compared to within the mixed layer, with a slightly more right-skewed
498 distribution (dashed black; Fig. 5c). Moderate MHWs (yellow curve) do not show a significant change in subsurface
499 chlorophyll ($\sim 0.25 \text{ mg m}^{-3}$) from non-MHWs. In contrast, strong MHWs exhibit a peak around 0.6 mg m^{-3} (orange
500 curve; Fig. 5c), reflecting elevated subsurface concentrations.

501
502 For ~~DOBOX~~ above the MLD, non-MHW periods show a bimodal distribution with the two main peaks at
503 approximately 180 and $220 \text{ } \mu\text{mol kg}^{-1}$, suggesting the presence of two types of oxygen regimes (Fig. 5b). The first
504 peak near $220 \text{ } \mu\text{mol kg}^{-1}$ remains stable across non-MHW, moderate and strong severity. Under strong MHWs, the
505 multi-modal structure remains, but the density between 185 – $195 \text{ } \mu\text{mol kg}^{-1}$ is enhanced relative to non-MHW
506 conditions, while density above $230 \text{ } \mu\text{mol kg}^{-1}$ is reduced. Additionally, a third peak appears near $165 \text{ } \mu\text{mol kg}^{-1}$ during
507 strong MHWs, which may reflect localized depletion of ~~DOBOX~~. These changes indicate that strong MHWs alter the
508 structure of ~~DOBOX~~ distribution above the MLD, indicating that strong MHWs are associated with a higher frequency
509 of low-oxygen values above the MLD and a relative reduction of high-oxygen values, although the multi-modal
510 structure largely reflects regional and seasonal regimes. As shown in Fig. S2, spring and summer exhibit generally
511 higher mixed layer DO compared to autumn, particularly in TAS and NSW, contributing to higher DO peak (~ 220
512 $\mu\text{mol kg}^{-1}$). In contrast, QLD, which has the largest number of MHW profiles (Fig. 2i), tends to show lower mixed
513 layer DO (Fig. S2), contributing more strongly to intermediate and lower DO density ranges.

514
515 For ~~DOBOX~~ below the MLD (Fig. 5d), the distributions slightly shift toward lower oxygen values under all conditions
516 compared to the layer above. During non-MHW periods, two peaks are observed at approximately 175 and $215 \text{ } \mu\text{mol}$
517 kg^{-1} . Under moderate MHWs, the distribution collapses into a single dominant peak near $\sim 205 \text{ } \mu\text{mol kg}^{-1}$, indicating a
518 homogenization of oxygen conditions below the MLD. Strong MHWs display an elevated lower peak at $180 \text{ } \mu\text{mol kg}^{-1}$,
519 similar to above the MLD, and a slightly reduced higher peak around $205 \text{ } \mu\text{mol kg}^{-1}$. Overall, the response of ~~DOBOX~~
520 to the severity of MHWs appears more heterogeneous and does not follow a uniform leftward shift.

521
522 Given that the results combine all regions and seasons, they may mask important regional and seasonal differences,
523 as well as sampling compositions. The following sections analyzeanalyze the vertical profiles of surface MHWs across
524 study regions and seasons to better understand their subsurface impacts on biogeochemical variables.

525

526

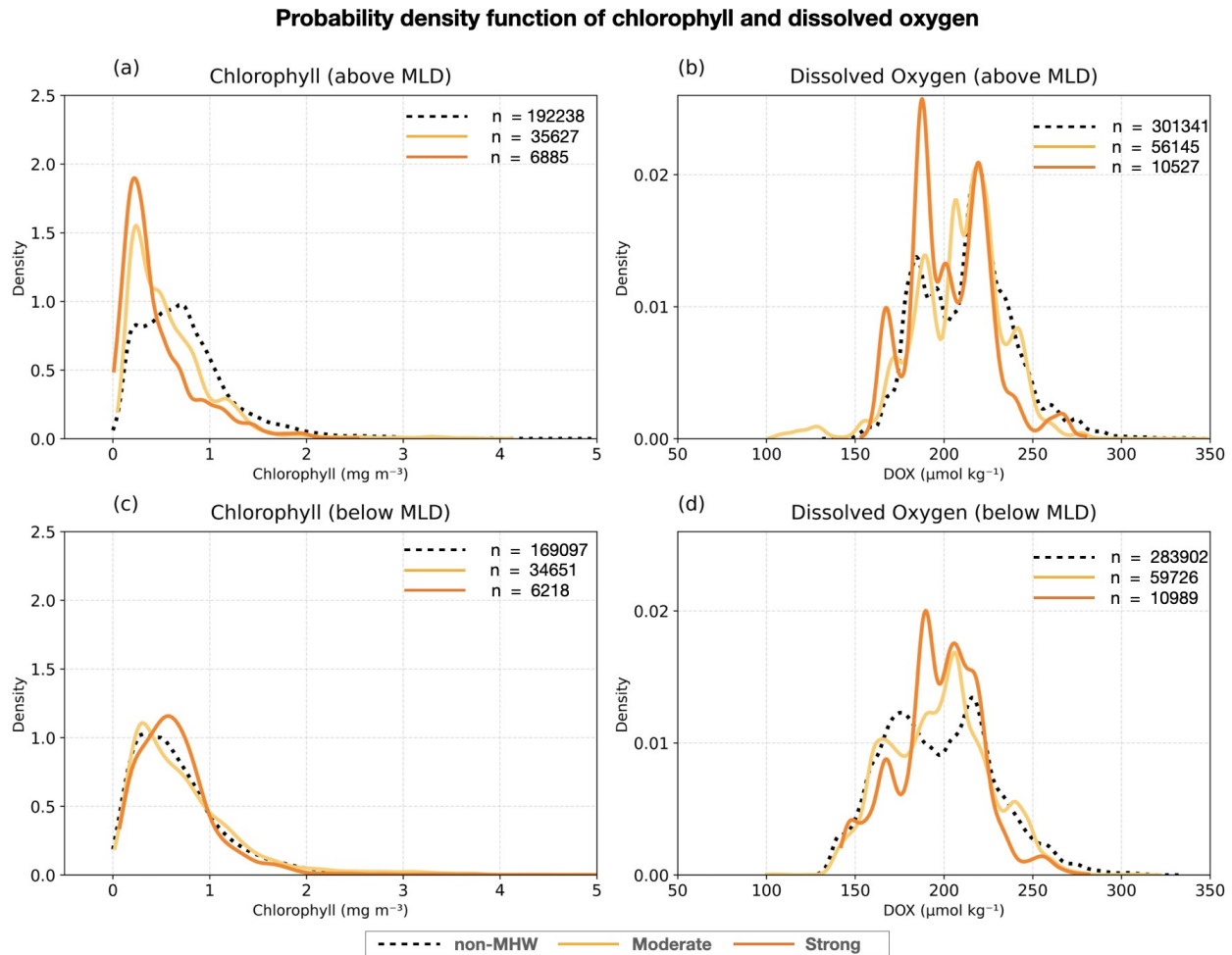
527

528

110

111

112



529

530 **Figure 5. Probability density function of (a, c) chlorophyll fluorescence (mg m^{-3}) and (b, d) dissolved oxygen ($\mu\text{mol kg}^{-1}$)**
 531 **above and below the MLD respectively, during MHWs (thick lines) for all regions. The distribution of chlorophyll and**
 532 **dissolved oxygen during MHWs are shown with severity index (S) categories: $1 < S \leq 2$ (Category 1: moderate; yellow**
 533 **curve), and $2 < S \leq 3$ (Category 2: strong; orange curve), while non-MHW ones are in black ($S \leq 1$; dashed curve). The**
 534 **number of samples (n) are indicated.**

535

536 3.3 Regional and seasonal changes in the water column

537 The vertical temperature structure of surface MHWs provides insight into how these events penetrate below the surface
 538 and interact with stratification and the mixed layer. These physical changes in the MLD, stratification, and MHW
 539 depth extent provide the context for examining chlorophyll variations throughout the water column and for assessing
 540 the depth of the DCM in particular seasons and regions. Changes in stratification directly affect phytoplankton
 541 productivity and oxygen concentrations, making it important to investigate how DOBOX responds to MHWs
 542 alongside chlorophyll. In general, DOBOX is highest at the surface due to diffusion from the atmosphere, decreasing

115

116

117

119
 543 with depth, and also varies with temperature through solubility. This vertical perspective sets the stage for comparing
 544 regional and seasonal patterns, to assess whether chlorophyll and DODOX responses to MHWs are consistent across
 545 Australia's continental shelf and how they are shaped by local seasonal oceanographic conditions (Figs. 6-9).

546

547 **3.3.1 Eastern Tasmania region: eddy-rich and a convergence zone**

548 Waters off eastern Tasmania (TAS) experience the convergence of warm, salty, and nutrient-poor subtropical waters
 549 from the southern extension of the EastEastern Australian Current (EAC) and cooler sub-Antarctic waters which lead
 550 to complex oceanographic conditions along the continental shelf. The intensification and southward extension of the
 551 EAC in the last few decades, associated with changes in the wind stress curl (Hill et al., 2008) and downstream
 552 propagating mesoscale eddies (Stammer et al., 2006). has altered stratification and vertical mixing (Holbrook and
 553 Bindoff, 1997; Ridgway, 2007; Oliver et al., 2017; Chiswell, 2023). This EAC extension and presence of eddies can,
 554 in fact, induce MHWs and These physical changes have implications for biogeochemical processes and overall
 555 ecosystem functioning (Zhao et al., 2022; in the region and during MHWs (Chiswell, 2023). From the glider
 556 observations, the vertical structure of temperature, salinity, chlorophyll and DODOX varied strongly within the
 557 seasons (Fig. 6). In the TAS region, glider profiles extended down to about 90 m and showed pronounced seasonal
 558 cycles in MLD and MHW depth extent. During summer MHWs, the MLD shoaled to about 18 m in summer (Fig. 6c),
 559 shallower than the seasonal composite mean MLD of non-mhwsmean, but extended to the bottom of the water column
 560 in winter (Fig. 6a). A similar pattern was reflected in the MHW depth extent, which decreased to about 2740 m in
 561 summer (Fig. S7) and deepened substantially in the other seasons (~66 m in spring; ~ 44 m in winter and autumn;
 562 using method D in Fig. S7). to the bottom of the water column in winter. The pronounced seasonality corresponded
 563 to variations in stratification, which peaked at about $7 \times 10^{-3} \text{ s}^{-2}$ near 30 m during summer (Fig. 6k), but was nearly
 564 absent in winter (Fig. 6i) and weakly stratifies in spring and autumn (Figs. 6j, l). Meanwhile, salinity values were
 565 consistently higher during MHWs all year round and throughout the water column compared to the seasonal mean
 566 composites derived from non-MHW conditionsmean conditions throughout the water column (Figs. 6 e-h), reflecting
 567 potential sources of higher saline waters coming onto the shelf from the EAC extension. This indicates that during
 568 MHWs, the shelf is influenced by warmer, saltier subtropical water masses associated with a strengthened or
 569 southward-shifted EAC, similar to conditions observed during the 2015/2016 Tasman Sea MHW (Oliver et al., 2017).
 570 The increased presence of these waters enhances upper-ocean density stratification, particularly in summer, which
 571 inhibits vertical mixing with the cooler, fresher sub-Antarctic waters. This is in agreement with the strong and
 572 statistically significant correlation ($r = 0.94$; Fig. 10) observed between MHW depth extent and the depth of maximum
 573 stratification during summer in TAS region.

574

575 Summer MHWs were marked by reduced chlorophyll at the surface relative to the seasonal composites during non-
 576 MHWs in the mixed layer (upper 20 m) but enhanced values at 40 m, exceeding 1.2 mg m^{-3} (Fig. 6o). During summer,
 577 the deepening of the DCM corresponded closely to the MHW depth extent and the depth of maximum stratification (r

120

121

122

123

124

578 = 0.40; Fig. 10). In other seasons, weaker stratification limited the development of strong DCMs both during MHWs
579 and under non-MHWs conditions. The MHW profile of DO in summer (Fig. 6s) showed a slightly higher
580 concentration in the upper 35 m relative to the seasonal composite mean profile of non-MHWs, exceeding 100%
581 saturation within this layer (Fig. S3). This suggests enhanced oxygen production in the mixed layer during MHWs,
582 consistent with the strong DCM through photosynthesis (Fig. S3). Similarly, in spring, MHWs showed slightly higher
583 DO and saturation levels (> 100%) in the upper 25 m than under non-MHW conditions, despite reduced chlorophyll.
584 This suggests that oxygen variability was not controlled by phytoplankton biomass but rather reflected supersaturation
585 due to ventilation. In contrast, during autumn and winter, the oxygen saturation level during MHWs was consistently
586 lower than non-MHW conditions throughout the water column due to weak stratification and reduced DCM, or
587 through solubility loss due to warming (Fig. S3), all of which limit phytoplankton productivity and oxygen production.

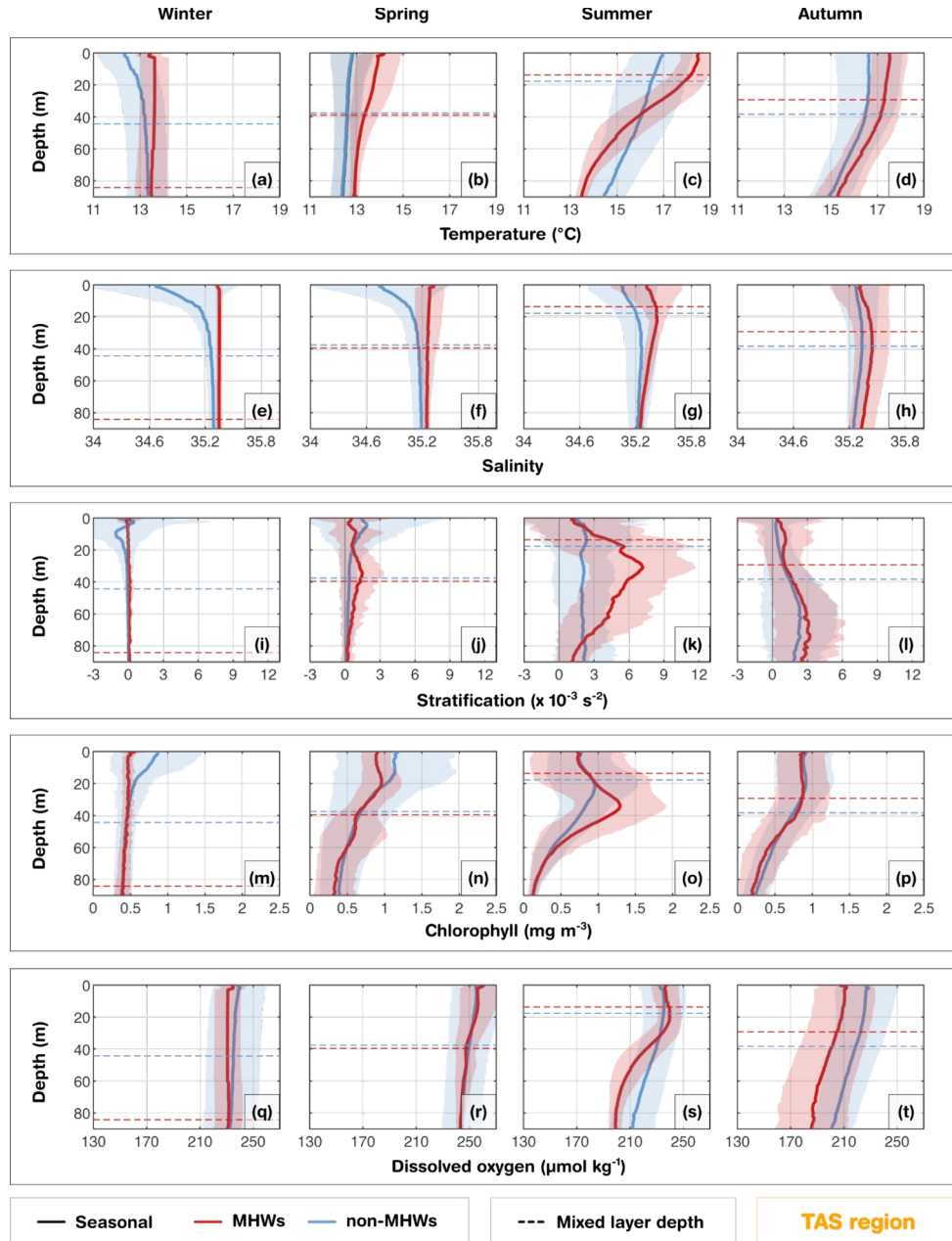
588

589 Summer MHWs were marked by reduced chlorophyll at the surface relative to the mean in the mixed layer (upper 20
590 m) but enhanced values at 40 m, exceeding 1.2 mg m^{-3} on average (Fig. 6o). During summer, the deepening of the
591 DCM corresponded closely to the MHW depth extent and the depth of maximum stratification. In other seasons,
592 weaker stratification limited the development of strong DCMs both during MHWs and under non-MHWs conditions.
593 The MHW profile of DOX in summer (Fig. 6s) showed a slightly higher concentration in the upper 35 m relative to
594 the mean profile, exceeding 100% saturation within this layer (Fig. S2). This suggests enhanced oxygen production
595 in the mixed layer during MHWs, consistent with the strong DCM, either through photosynthesis, or through mixing
596 (Fig. S2). Similarly, in spring, MHWs showed slightly higher DOX than non-MHW conditions in the upper 25 m. In
597 contrast, during autumn and winter, DOX during MHWs was consistently lower than the mean conditions throughout
598 the water column due to weak stratification and reduced DCM, or through solubility loss due to warming (Fig. S2),
599 all of which limit phytoplankton productivity and oxygen production.

125

126

127



600

601 Figure 6. Tasmania region (TAS): Seasonal composite mean profiles Profiles of (a-d) temperature ($^{\circ}\text{C}$), (e-h) salinity (PSU),602 (i-l) stratification ($\times 10^{-3} \text{ s}^{-2}$), (m-p) chlorophyll (mg m^{-3}) and (q-t) dissolved oxygen ($\mu\text{mol kg}^{-1}$) averaged for all seasonal603 profiles (black), MHW events (red), and non-MHW events (blue). Horizontal dashed lines indicate the corresponding604 seasonal composite mean MLDs for are the mean mixed layer depths for the season, MHWs and non-MHWs. Shaded areas

605 represent the respective standard deviations. Seasons are defined as winter (June-August), spring (September-November),

606 summer (December-February), and autumn (March-May).

130

131

132

133

134

607

608 3.3.2 New South Wales region: narrow shelf and boundary current influence

609 In the New South Wales (NSW) region, the narrow continental shelf waters are shaped by the warm EAC, which
610 contributes to mixing and transports warm nutrient-poor waters onto the shelf when it meanders or shifts inshore. The
611 intrusions of the EAC increases the likelihood of full-depth extended MHWs, which are longer and dominant in winter
612 (Schaeffer et al., 2017, 2023). In this region, seasonal winds and stratification also strongly influence MHWs' depth
613 structure and development, especially in summer (Schaeffer and Roughan, 2017). In the glider observations, during
614 MHWs, warm anomalies were confined to slightly shallower depths (~35 m; Fig. S740-m) in winter and (~33 m; Fig.
615 S7) autumn, compared to deeper depths in austral summer (~47 m; Fig. S745-50 m) and extended-deepest-in-spring
616 (~46 m; Fig. S7400-m). Salinity showed no significant change during MHWs and remained relatively stable
617 throughout the water column throughout the year (Figs. 7e-h). Although waters off NSW are generally more stratified
618 in summer than winter, stratification further intensified and deepened during MHWs in all seasons, reaching $\sim 12 \times 10^3$
619 s^{-2} at 30-40 m in summer and $\sim 3 \times 10^3 s^{-2}$ at 45 m in winter, closely matching the depth extent of MHWs (Figs. 7i,k;
620 S7; 10).

621

622 The ~~DCM chlorophyll vertical structure and magnitude~~ experienced strong seasonality. Across all seasons, surface
623 chlorophyll concentrations were reduced during MHWs, while increasing at ~20-40 m (exceeding 1 mg m^{-3}) during
624 spring, ~~summer and autumn~~ and ~~summer~~ (Figs. 7n-p). These chlorophyll maxima were deeper and stronger than
625 under non-MHW conditions, and their depth aligned well with both maximum stratification and the MHW depth
626 extent (Fig. S7). In contrast, during ~~autumn and~~ winter, weaker stratification corresponded ~~to~~ shallower or absent
627 DCMs, with chlorophyll concentrations below 1 mg m^{-3} (Figs. 7m-p).

628

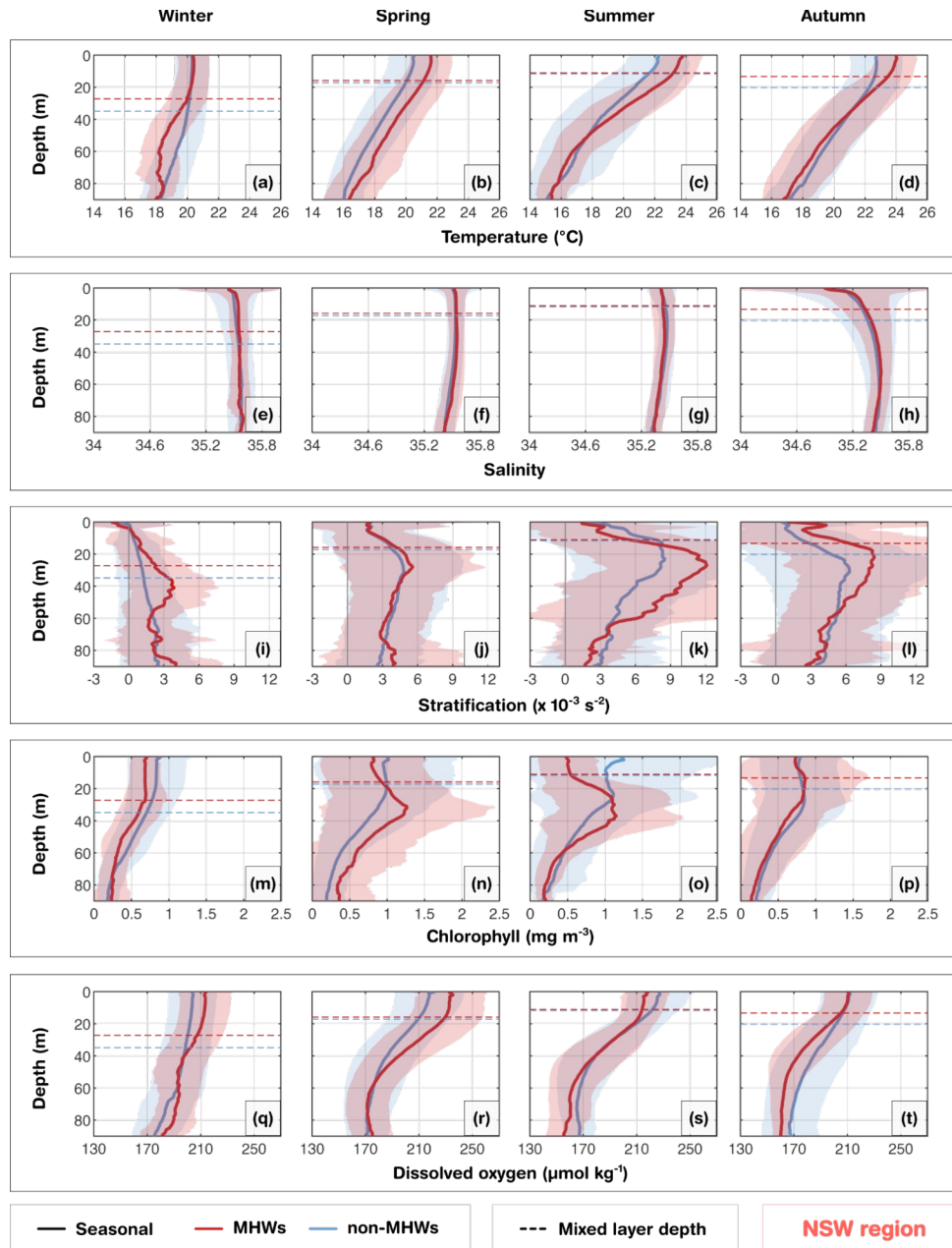
629 In summer, MHWs were associated with reduced ~~DO~~ in the upper 20 m, ~~likely due to warming-induced reduced~~
630 ~~solubility and below 50 m~~ (Fig. S37s). At intermediate depths, a more pronounced DCM was present (Fig. 7o). ~~Further~~
631 ~~deoxygenation below 50 m may result from enhanced respiration of sinking organic matter from the intermediate~~
632 ~~layer~~. However, little difference in ~~DO~~ levels from non-MHW conditions ~~in the intermediate layer~~ indicated that
633 photosynthesis was insufficient to alter the total mean ~~DO~~ (Fig. S3DOX (Fig S2)). Conversely, in spring, MHWs were
634 associated with higher ~~DO~~ concentrations in the upper 50 m, exceeding 100% saturation relative to non-MHW
635 conditions within the mixed layer (Fig. S3S2). This ~~DO~~ enhancement during spring is consistent with strong
636 stratification and deep DCM (Figs. 7j,n,r), and is likely driven by photosynthesis, mixing or advection of oxygen-rich
637 waters. Moreover, north-eastward winds in spring (Wood et al., 2016), favour downwelling of warmer surface waters,
638 contributing to the deep extent of MHWs in spring (Fig. 7b) and transporting oxygen to deeper layers. By contrast,
639 in autumn, ~~DO~~ concentrations were similar within the mixed layer but decreased below the MLD (Fig. 7t),
640 ~~consistent with a DCM positioned higher in the water column (Fig. 7l; Fig-S2)~~.

641

135

136

137



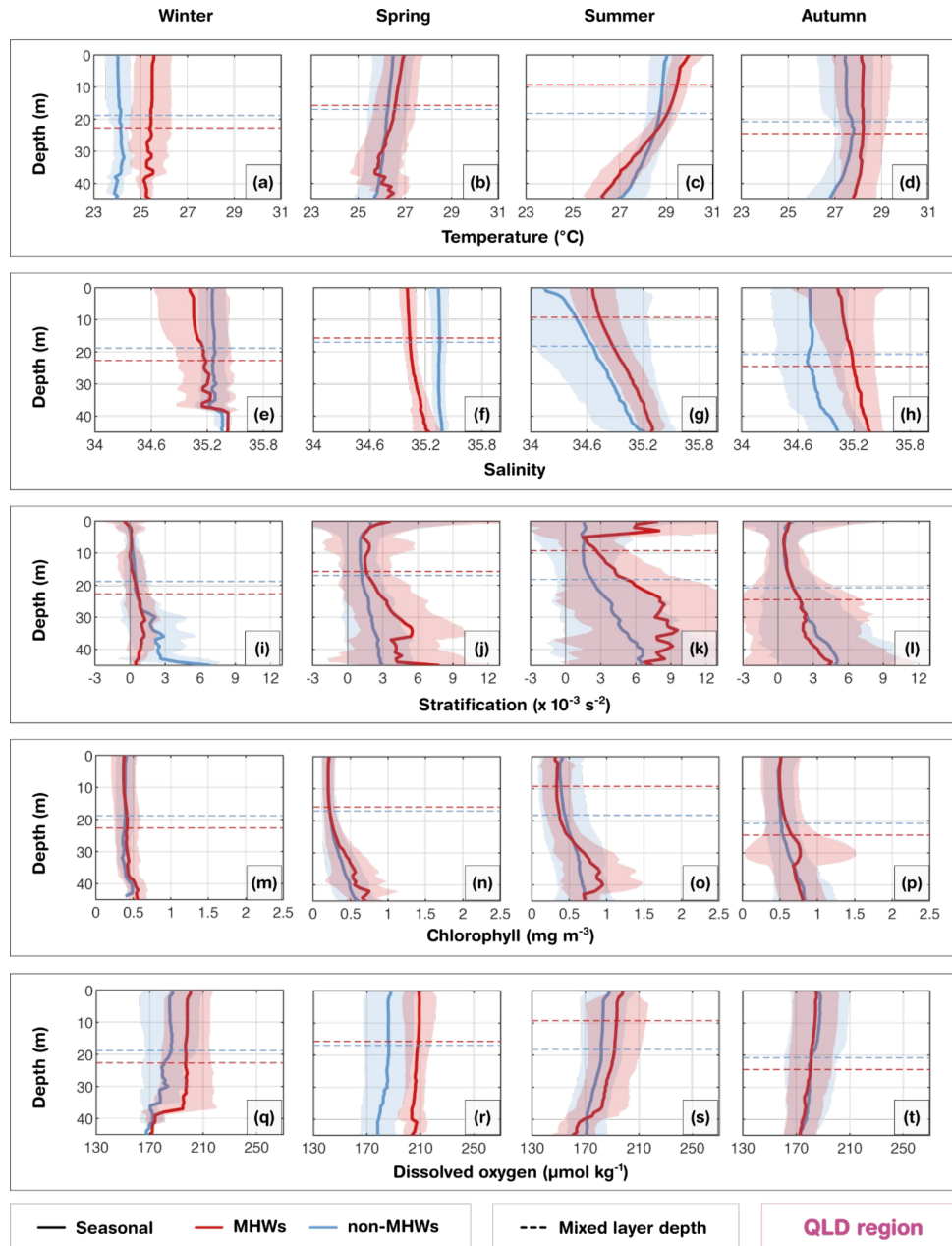
642
 643 Figure 7. Same as Fig. 6, but for the New South Wales (NSW) region.
 644

645 | 3.3.3 Queensland region: shallow shelf and biologically active area

646 | The Queensland (QLD) region is home to the GBR Great Barrier Reef, which has a shallow continental shelf with
 647 coral reefs and reef passages and the shelf circulation is influenced by the Gulf of Papua Current (in the north), East
 648 Australian Current (EAC; from the central sector to south), the Coral Sea circulation, riverine inputs and wind-driven
 649 processes (Ridgway et al., 2018; Benthuisen et al., 2022; Wolanski and Kingsford, 2024). The seasonal composite

144
 650 ~~mean evolution~~ of MLD and the MHW depth extent largely followed the seasonal cycle (Figs. 8; S7Fig-8). During
 651 summer MHWs, the MLD shoaled to 9 m ~~consistent with a shallow~~, the MHW depth extent (~19m; Fig. S7) ~~reached~~
 652 ~~25 m~~, and ~~strong stratification peaking above 9~~ ~~the stratification peaked above~~ $10 \times 10^{-3} \text{ s}^{-2}$ at ~~the surface~~ (Fig. 8k). ~~The~~
 653 ~~35–45 m~~. This intense near-surface stratification is likely exacerbated by the formation of barrier layers during the
 654 wet season (Schroeder et al., 2012), where riverine freshwater input and precipitation create a buoyant low-salinity
 655 lens (Fig. 8g) and subsurface intrusive upwelling through reef passages brings saltier Coral Sea waters below
 656 (Benthuisen et al. 2016). These barrier layers inhibit vertical mixing, effectively trapping heat in the surface layer and
 657 intensifying the MHW magnitude. In contrast, during winter ~~and autumn~~ MHWs, the MLD deepened to 23 m ~~and 25~~
 658 ~~m respectively, consistent with a deepening of the~~, the MHW depth extent ~~reached about 40 m and stratification~~
 659 ~~weakened to less than $2 \times 10^{-3} \text{ s}^{-2}$~~ . The MHW depth extent ~~to about 22 m and 27 m respectively~~ (Fig. S7). ~~During these~~
 660 ~~seasons, the stratification weakened to less than 3~~ ~~reached deeper depths in both autumn and spring (at least 45 m,~~
 661 ~~which is the depth of our mean profiles), coinciding with strong stratification over $5 \times 10^{-3} \text{ s}^{-2}$ at similar depths~~. Although
 662 fresher waters were observed near the surface in winter and spring, salinity values were not as low as in summer, and
 663 the vertical salinity gradient was not as pronounced as in summer and autumn, suggesting the dominance of wind-
 664 driven and convective mixing in homogenizing the water column during these cooler seasons.

665
 666 Biologically, the strong physical stratification during summer MHWs shaped the vertical chlorophyll structure. The
 667 DCM reached 1 mg m^{-3} at 40 m (Fig. 8o), coinciding with strong fluctuations in stratification levels below 30 m,
 668 acting as a productive interface where light and nutrient availability overlap. Although less pronounced than summer,
 669 autumn also displayed high chlorophyll concentrations exceeding 0.9 mg m^{-3} at 30 m. ~~However, chlorophyll~~
 670 ~~concentration during MHWs in the upper 20 m remained lower than the seasonal composites, indicating reduced~~
 671 ~~productivity in the upper layers. The increased chlorophyll pattern observed in the subsurface layer may reflect the~~
 672 ~~seasonal transition toward weaker~~, ~~suggesting that residual stratification and associated nutrient entrainment~~
 673 ~~sustaining subsurface productivity from deeper waters during the autumn MHWs~~ ~~nutrient availability still supported~~
 674 ~~high productivity at depth following the summer bloom period~~. In contrast, winter and spring MHWs showed a weaker
 675 coupling between stratification and chlorophyll ~~than the other seasons~~, consistent with enhanced mixing. The ~~DO~~
 676 ~~DO~~ during MHWs compared to ~~non-MHW conditions~~ ~~the mean~~ were consistently higher throughout the shallow water
 677 column (except in autumn). This presents a ~~counterintuitive thermodynamic behaviour~~ ~~thermodynamic anomaly~~, as
 678 warmer water typically holds less dissolved gas. Consequently, the observed ~~DO increase during summer, and spring~~
 679 ~~increase~~ indicates that biological oxygen production (photosynthesis) was sufficient to offset the physical solubility
 680 loss induced by warming (Fig. S3S2). While biological production dominates the summer signal, the higher ~~DO~~
 681 ~~DO~~ observed during MHWs in winter ~~and spring~~ may be related to seasonal ventilation that drives the deep vertical extent
 682 of temperature anomalies, leading to higher oxygen levels than normal. In contrast, the lower ~~DO~~
 683 ~~DO~~ in autumn, despite the presence of subsurface chlorophyll, ~~appears to be dominated by enhanced~~ ~~likely reflect a post-~~
 684 ~~bloom phase where~~ respiration rates ~~increased~~, consuming oxygen as organic matter from ~~prior blooms~~. ~~In addition to~~



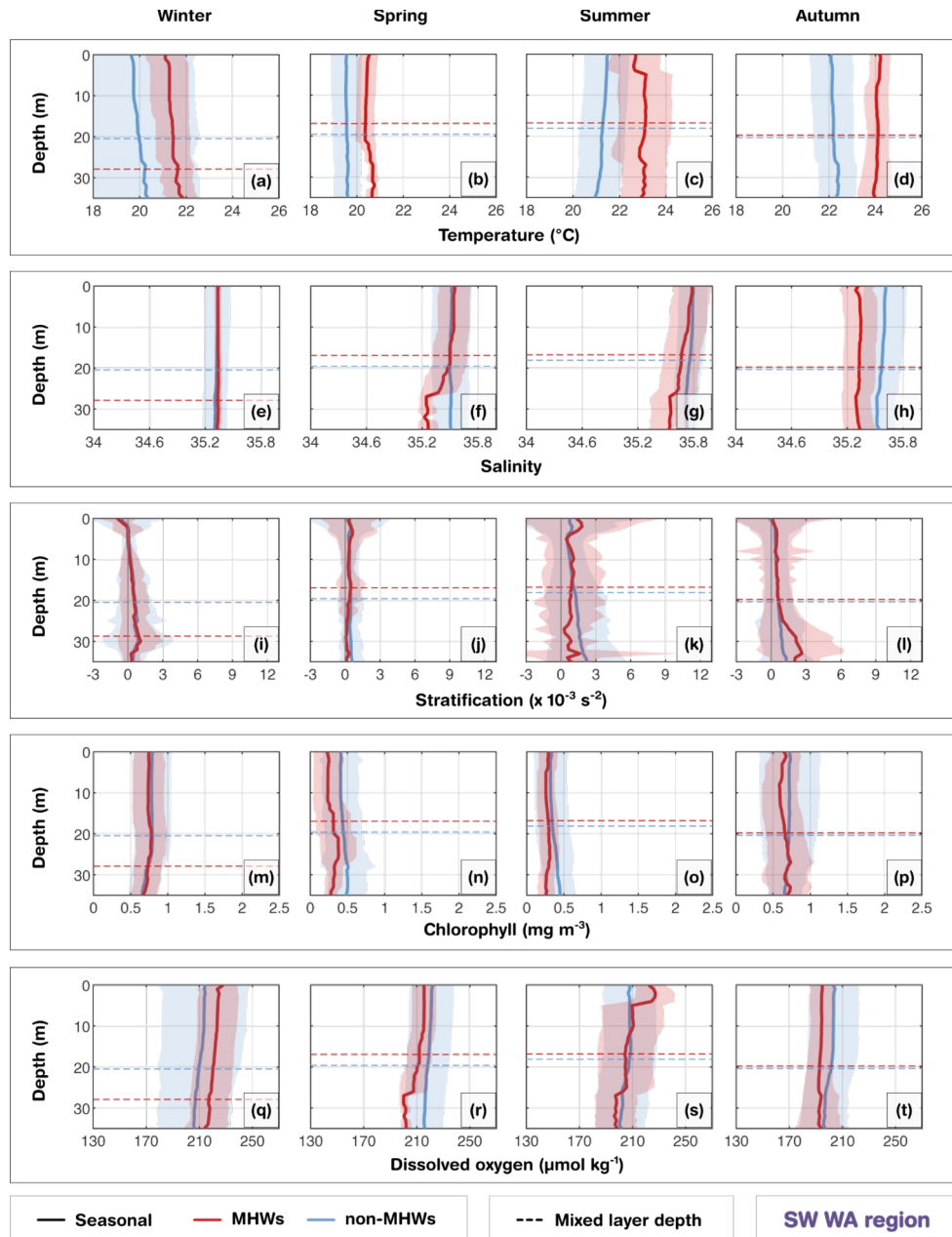
690 **3.3.4 Southwest Western Australia region: shallow shelf and oligotrophic conditions**

691 The southwest Western Australia (SW WA) region is characterised by a shallow shelf dominated by the warm, fresh

692 poleward-flowing Leeuwin Current, maintaining oligotrophic conditions, while the Capes Current emerges inshore

154
693 during spring and summer months with upwelling leading to phytoplankton blooms (Hanson et al., 2005, Feng et al.,
694 2025). The gliders were sampled over this coastal region, where the shelf narrows from ~50 km to 20 km (Fig. 1e;
695 Brooke et al., 2010). From the coast to the mid-shelf, waters had weaker stratification in the upper 40 m (Figs. 9i-j)
696 compared with other regions, where the small temperature inversion in autumn and winter is consistent with an annual
697 climatology from nearby mooring measurements (Feng et al., 2025). Unlike the stratified systems in eastern Australia,
698 this weak stratification coupled with the dominance of the Leeuwin Current drives downwelling-favorable conditions
699 that facilitate the rapid vertical propagation of surface heat anomalies. As a result, during surface MHWs, anomalously
700 warm surface temperatures extended further deep in all seasons, following the seasonal cycle of the MLD throughout
701 the depth of our mean profiles (40 m) in all seasons, leading to ~+1–2°C differences in the mean temperature profiles
702 compared with non-MHW conditions (Figs. 9a-d). The MLD shoaled during summer MHWs compared to non-MHW
703 conditions, in contrast to a deepening during winter MHWs while the MLD was deeper during MHWs in winter. In
704 autumn, the MHW conditions were warmer and fresher than non-MHWs, potentially in part related to sampling during
705 the 2011 Ningaloo Niño (Fig. 4d4b), when glider measurements were concentrated around 31.5–32° S. During this
706 extreme event, low salinity anomalies were transported by the Leeuwin Current and were some of the lowest recorded
707 values since the 1950s (Feng et al., 2015). This highlights that severe MHWs in this region are largely advection-
708 driven events, where the transport of buoyant, low-salinity tropical waters enhances the density contrast with offshore
709 waters, further trapping heat against the coast.

710
711 ~~Biogeochemically, the strong advective nature of these MHWs exerts a controlling influence on shelf productivity.~~
712 ~~During surface MHWs, shelf waters had lower chlorophyll concentrations during spring (Fig. 9n). Surface MHWs~~
713 ~~were associated with anomalously high DOX during summer and winter reflecting seasonal ventilation (Fig. S2)~~
714 ~~facilitated by the weak stratification, which allows atmospheric oxygen to mix effectively throughout the water~~
715 ~~column. However, significantly lower DOX levels were observed in spring and autumn (Figs. 9r, t). In autumn, with~~
716 ~~sampling through the 2011 Ningaloo Niño, the relatively reduced near-surface chlorophyll and DOX might reflect~~
717 ~~equatorward influences on this region, as offshore waters to the north have been recorded with lower chlorophyll and~~
718 ~~DOX (e.g. Woo and Pattiaratchi, 2008; Weller et al., 2011). This reduction suggests a decoupling from the solubility-~~
719 ~~driven pattern seen in other regions, pointing instead to the physical advection of warm, nutrient-poor, and oxygen-~~
720 ~~depleted tropical waters by the intensified Leeuwin Current, which suppresses local productivity and Capes Current~~
721 ~~upwelling. These results reveal that, in the upper 40 m of coastal waters off SW WA, reduced stratification influences~~
722 ~~the vertical structure of chlorophyll and DOX, even during surface MHWs, and they could be affected by latitudinal~~
723 ~~transport of water properties, as has been found during marine heatwaves caused by a Leeuwin Current intensification.~~
724



725

726 **Figure 9. Same as Fig. 6, but for the southwest Western Australia (SW WA) region.**

727

728 Biogeochemically, the strong advective nature of these MHWs exerts a controlling influence on shelf productivity.729 During surface MHWs, shelf waters had lower chlorophyll concentrations than non-MHWs (Fig. 9m-p). Surface730 MHWs were associated with anomalously high oxygen saturation levels (>100%), higher than non-MHW conditions731 during summer and winter. In summer, this likely reflects biological production in the upper layers due to shallower732 MLD while in winter, it may be partially influenced by enhanced ventilation (Fig. S3). Weak stratification facilitates733 this supersaturation by allowing atmospheric oxygen to mix effectively throughout the water column, even if dissolved

160

161

162

163

164

734 oxygen is not substantially higher than non-MHW conditions. However, significantly lower DO levels were observed
735 in spring and autumn (Figs. 9r, t). In autumn, with sampling through the 2011 Ningaloo Niño, the relatively reduced
736 near-surface chlorophyll and DO might reflect equatorward influences on this region, as offshore waters to the north
737 have been recorded with lower chlorophyll and DO (e.g. Woo and Pattiaratchi, 2008; Weller et al., 2011). This
738 reduction suggests a decoupling from the solubility-driven pattern seen in other regions, pointing instead to the
739 physical advection of warm, nutrient-poor, and oxygen-depleted tropical waters by the intensified Leeuwin Current,
740 which suppresses local productivity and Capes Current upwelling. These results reveal that, in the upper 40 m of
741 coastal waters off SW WA, reduced stratification influences the vertical structure of chlorophyll and DO (Fig. 10),
742 even during surface MHWs, and they could be affected by latitudinal transport of water properties, as has been found
743 during MHWs caused by a Leeuwin Current intensification.

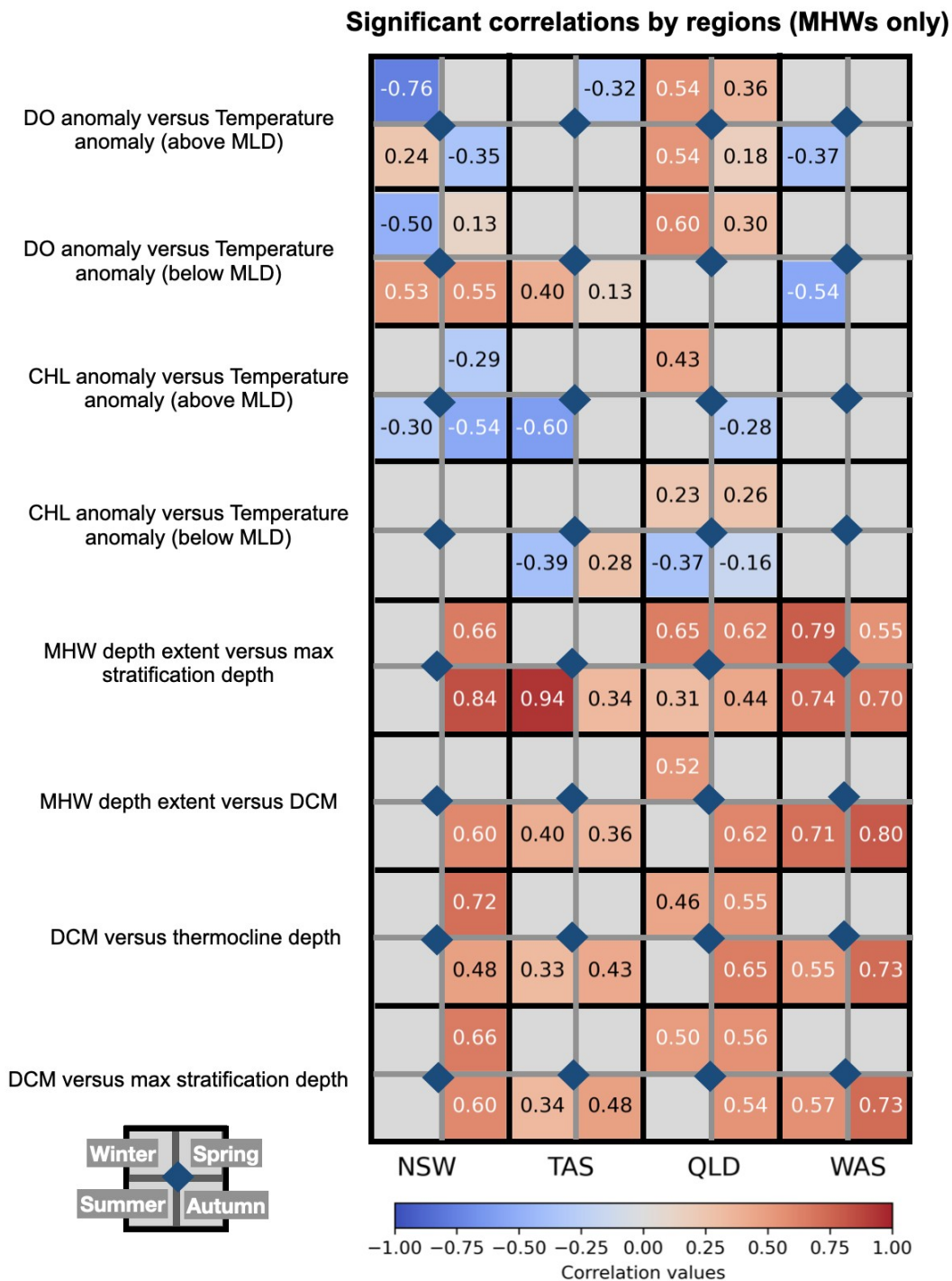
744

745

165

166

167



746

747 **Figure 10. Synthesis figure of seasonal correlations between key physical-biogeochemical variables during MHWs across**
 748 **four regions (NSW, TAS, QLD, SW WA). Rows correspond to variable pairs: (1) dissolved oxygen anomalies (DO) versus**
 749 **temperature anomalies (above the MLD), (2) dissolved oxygen anomalies (DO) versus temperature anomalies (below the**
 750 **MLD), (3) chlorophyll anomalies versus temperature anomalies (above the MLD), (4) chlorophyll anomalies versus**
 751 **temperature anomalies (below the MLD), (5) MHW depth extent versus depth of maximum stratification, (6) MHW depth**

170

171

172

173

174

752 extent versus deep DCM depth, (7) DCM depth versus thermocline depth, and (8) DCM depth versus depth of maximum
753 stratification. Columns correspond to regions. Each cell is subdivided into four seasonal quadrants, colored by the Pearson
754 correlation coefficient (r) values with values indicated within each quadrant.

755 **4. Discussion**

756 MHWs have been extensively documented around Australia, yet their impact on subsurface biogeochemical variables
757 remains a critical gap in our understanding due to limited long-term observations. We used satellite sea surface
758 temperature and up to 16 years of glider observations across four contrasting and well-observed coastal regions:
759 eastern Tasmania (TAS), New South Wales (NSW), Queensland (QLD), and southwest Western Australia (SW WA).
760 Our study reveals how surface MHWs alter, seasonally, the subsurface temperature, stratification, and biogeochemical
761 variables (chlorophyll and dissolved oxygen). These findings provide new insights into region-specific responses,
762 which help fill critical gaps in understanding the subsurface impacts of MHWs along the continental shelf of Australia.
763 -

764 Each shelf region around Australia has experienced impactful MHWs linked to atmospheric forcing (Schaeffer and
765 Roughan, 2017; Wang et al., 2023; Gregory et al., 2023; Huang et al., 2024) and regional circulation patterns,
766 including boundary current intensification. The Tasman Sea has been identified as a global warming hotspot,
767 experiencing the strongest warming in the Southern Hemisphere (Holbrook and Bindoff, 1997; Hobday and Peel,
768 2014); yet biogeochemical data documenting shelf water responses to MHWs remain scarce. The unprecedented
769 MHW observed in 2015/16 off Tasmania (captured by a glider mission) led to a wide range of ecological impacts
770 (Oliver et al., 2017), driven by enhanced eddy kinetic energy associated with a strengthened southward extension of
771 the East Australian Current (Oliver et al., 2017).

772

773 Off NSW, two glider missions recorded abrupt yet severe MHWs during spring 2013 and 2018, each reaching a
774 severity index of 3 (based on satellite SST data) and posing severe risks to the shelf ecosystems. MHWs on the NSW
775 continental shelf have been classified from mooring observations (Schaeffer et al., 2023) as shallow (air-sea flux
776 driven), extended through the water column (linked to the intrusion of the EAC), or sub-surface only (linked to
777 downwelling winds). However, these types of MHWs have not been linked to biogeochemical characteristics yet. In
778 South Australia, the 2013 MHW offers insight into possible impacts in surrounding regions. There, the widespread
779 MHW triggered harmful algal blooms, resulting in massive fish and abalone mortality, driven by hypoxia and related
780 physiological stress (Roberts et al., 2019).

781

782 **4. Discussion**

783 MHWs have been extensively documented around Australia, yet their impact on subsurface biogeochemical variables
784 remains a critical gap in our understanding due to limited long-term observations. We used satellite SST and up to 16
785 years of glider observations across four contrasting and well-observed coastal regions: eastern Tasmania (TAS), New
786 South Wales (NSW), Queensland (QLD), and southwest Western Australia (SW WA). Our study reveals how surface

175

176

177

179 MHWs alter, seasonally, the subsurface temperature, salinity, stratification, and biogeochemical variables (chlorophyll
180 and dissolved oxygen). These findings provide new insights into region-specific responses, which help fill critical
181 gaps in understanding the subsurface impacts of MHWs along the continental shelf of Australia.

182 Off QLD, the Great Barrier Reef (GBR), the world's largest coral reef system, has suffered repeated MHW-induced
183 coral bleaching events, with six mass coral bleaching events between 2016 and 2025 (e.g. Great Barrier Reef Marine
184 Park Authority et al. 2025). In fact, the event in 2016 was well captured by three glider missions, reaching an MHW
185 severity index of 2.6 (indicative of strong category). Similarly, the 2020 MHW in the GBR and Coral Sea caused
186 widespread coral bleaching, with glider missions recording severity values exceeding 2, consistent with observations
187 reported by Benthuisen et al. (2021). These extreme events were associated with weak wind stress, reduced cloud
188 cover, and anomalous heat transport (Berkelmans and Oliver, 1999; Schiller et al., 2009; Benthuisen et al., 2018,
189 2021).

190 Across most regions, the vertical structure of temperature, salinity, and stratification displayed strong seasonality, with
191 shallow mixed layers and enhanced stratification in summer, and deeper, weaker stratification in winter. During
192 MHWs, these patterns tend to be intensified, with shallower MLD and stronger stratification in summer, and deeper
193 MLD in winter (except in NSW). During winter MHWs, the water column is already weakly stratified, and warming
194 alone does not generate a strong density gradient to shoal the MLD. In addition, anomalous processes associated with
195 winter MHWs, such as wind-driven mixing and horizontal advection, can further deepen the MLD relative to typical
196 winter conditions. In some regions, such as Western Australia, Leeuwin Current-driven MHWs produce deep warming
197 that can result in a deep MHW structure (Zhang et al., 2023), where warmer water penetrates to greater depths, thereby
198 leading to deeper MLD during MHW winters. In contrast, NSW did not exhibit this deepening of the MLD during
199 winter MHWs due to the hydrography of the EAC which dominates the NSW shelf year-round. Unlike other regions,
200 stratification in NSW is not driven purely by seasonal heating and cooling but is strongly modulated by shelf
201 encroachment of the EAC, mesoscale eddies, and current instabilities. This persistent influence also shapes the
202 seasonality of phytoplankton in NSW, with summer-spring biomass maxima and reduced winter abundance (Schaeffer
203 et al, 2015), consistent with our findings. SW WA exhibited particularly minimal stratification changes due to its
204 naturally well-mixed conditions, however, transient increases in stratification can occur during periods of wind
205 relaxation or fluctuations in the Leuwin or Capes Currents. The MHW depth extent was shallower in strongly
206 stratified (summer) conditions and deeper during winter when the water column was more homogeneous. These results
207 align well with Schaeffer and Roughan (2017) and with hypothesis (3) that the vertical depth extent of surface MHWs
208 vary seasonally according to background stratification and hydrography.

209 Off SW WA, the shelf is shallow, and the poleward-flowing Leeuwin Current transport warm, nutrient-poor tropical
210 waters southward (Chen et al., 2020), suppressing upwelling and maintaining oligotrophic, vertically homogeneous
211 conditions. The 2011 MHW was triggered by a La Niña-intensified Leeuwin Current (Feng et al., 2013; Benthuisen
212 et al., 2014), resulting in reduced DOX (Rose et al., 2012), decline in chlorophyll-based productivity (Richardson et
213 al., 2020) and severe ecological and economic consequences (Pearce et al., 2011; Rose et al., 2012). This major MHW

183

184

823 (severity index 2.1) was captured by two glider missions (Fig. 4), highlighting the need for continued subsurface
824 MHW monitoring beyond satellite observations.

825

826 Chlorophyll responses are tightly coupled to MHW severity and regional hydrography. Results showed that surface
827 chlorophyll above the MLD overall declines with increasing MHW severity, in line with previous studies (Le Grix et
828 al., 2020; Sen Gupta et al., 2020; Gruber et al., 2021). This finding supports hypothesis (4) that the severity of MHW
829 modulates chlorophyll concentration and is also consistent with hypothesis (1) that surface MHWs generally reduce
830 chlorophyll concentrations in the mixed layer. The observed decline in surface chlorophyll with increasing severity is
831 likely driven by enhanced stratification and reduced nutrient supply from the subsurface which limit surface
832 phytoplankton growth during MHWs. This pattern is evident in the correlation plots (Figs. 10 and S4), which reveal
833 an overall negative relationship between temperature and chlorophyll anomalies above the MLD, except in SW WA
834 where limited sampling may affect the correlation (Fig. S8).

835 Across most regions, the vertical structure of temperature, salinity, and stratification displayed strong seasonality, with
836 shallow mixed layers and enhanced stratification in summer, and deeper, weaker stratification in winter. During
837 MHWs, these patterns tend to be intensified, with shallower MLD and stronger stratification in summer, and deeper
838 MLD in winter (except in NSW). SW WA exhibited particularly minimal stratification changes due to its naturally
839 well-mixed conditions. The MHW depth extent was shallower in strongly stratified (summer) conditions and deeper
840 during winter when the water column was more homogeneous. These results align with Schaeffer and Roughan (2017),
841 emphasizing the role of stratification and regional hydrography in shaping MHW vertical structure.

842

843 Subsurface chlorophyll distributions during MHWs has been a topic of incipient discussion. Here, our study showed
844 evidence for increased chlorophyll below the MLD during strong MHWs along the Australian continental shelves,
845 pointing to the formation of a sharper and deeper DCM in spring, summer and autumn due to enhanced stratification
846 (except in the oligotrophic region of Western Australia). This finding supports hypothesis (2), indicating that despite
847 surface reductions, MHWs can promote deeper chlorophyll maxima and enhanced subsurface productivity. Although
848 the surface becomes nutrient-poor, the shoaling of the MLD during MHWs increases phytoplankton exposure to higher
849 light intensities, thereby allowing phytoplankton to thrive at depth (e.g. Hayashida et al., 2020). DCM depth correlated
850 strongly with the depth of maximum stratification in NSW (Pearson correlation coefficient, $r = 0.66$ in spring, $r = 0.60$
851 in autumn), in TAS ($r = 0.48$ in autumn), in QLD ($r = 0.56$ in Spring) and SW WA ($r = 0.73$ in autumn), all statistically
852 significant. We also found strong correlations between DCM depth and MHW extent, in NSW ($r = 0.60$ in autumn),
853 QLD ($r = 0.62$ in autumn, $r = 0.52$ in winter) and SW WA ($r = 0.71$ in summer, $r = 0.80$ in autumn). This finding is
854 consistent with Ma and Chen (2025), who showed that MHWs promote DCM development at the global scale. In
855 contrast, in winter or in vertically-mixed upper ocean waters, MHWs penetrate to depth, eroding stratification and
856 suppressing DCM. The level of stratification controls the thermocline depth, which we found to be strongly correlated
857 with DCM depth (Figs.10 and S4), and thereby governs both the vertical position of the DCM and the MHW depth

185

186

187

189
858 extent. Our results support hypothesis (3) that regional hydrography and seasonal stratification control the vertical
859 extent of MHWs.

860 Chlorophyll responses are tightly coupled to MHW severity and regional hydrography. Results showed that surface
861 chlorophyll above the MLD overall declines with increasing MHW severity, in line with previous studies (Le Grix et
862 al., 2020; Sen Gupta et al., 2020; Gruber et al., 2021) and support the hypothesis that enhanced stratification and
863 reduced nutrient supply from the subsurface limit surface phytoplankton growth during these events. This pattern is
864 evident in the correlation plots (Figs. 10 and S3), which reveal an overall negative relationship between temperature
865 and chlorophyll anomalies above the MLD, except in SW WA where limited sampling may affect the correlation (Fig.
866 S6).

867
868 DO responses to MHW and their severity are less straightforward. Australia's surrounding waters exhibit distinct
869 oxygen regimes due to contrasting water masses, biogeochemical environments and seasonal variability. Low-oxygen
870 regimes are usually present in tropical and subtropical regions (Paulmier and Ruiz-Pino, 2009; Davila et al., 2023)
871 such as QLD and SW WA, influenced by oxygen-poor water masses, while high-oxygen regimes are found in
872 temperate regions (NSW, TAS), dominated by well-ventilated waters. During strong MHWs, low-oxygen regimes
873 may become further deoxygenated in the MLD (Figs. S2, S3), such as in QLD, due to enhanced stratification and
874 reduced vertical ventilation, consistent with hypothesis (1) that MHWs reduce dissolved oxygen in the mixed layer
875 and hypothesis (4) that MHW severity modulates dissolved oxygen variability. Although reduced upwelling can limit
876 the entrainment of oxygen-poor subsurface waters, it also restricts the supply of oxygen from deeper layers and reduces
877 mixing, isolating the mixed layer. In shallow coastal regions, elevated temperatures further decrease solubility, and
878 may increase the biological oxygen demand. Besides temperature's direct effect on oxygen solubility, changes in DO
879 arise from complex interactions between circulation and stratification, and primary productivity (Gruber, 2011; Gruber
880 et al., 2021).

881 Subsurface chlorophyll distributions during MHWs has been a topic of incipient discussion. Here, our study showed
882 evidence for increased chlorophyll below the MLD during strong MHWs along the Australian continental shelves,
883 pointing to the formation of a sharper and deeper DCM in particular seasons. This finding supports hypothesis (2),
884 indicating that despite surface reductions, MHWs can promote deeper chlorophyll maxima and enhanced subsurface
885 productivity. Although the surface becomes nutrient poor, light still penetrates deeper during MHWs because the
886 MLD becomes shallower, therefore allowing phytoplankton to thrive at depth (e.g. Hayashida and Stratton, 2020).
887 DCM depth correlated strongly with the depth of maximum stratification (Pearson correlation coefficient, $r = 0.73$ in
888 NSW summer, and $r = 0.57$ in SW WA autumn; all statistically significant). We also found strong correlations between
889 DCM depth and MHW extent, with the highest values in NSW ($r = 0.86$ in summer, $r = 0.70$ in autumn and $r = 0.63$
890 in spring), followed by significant correlations in TAS ($r = 0.60$ in summer), and QLD ($r = 0.60$ in autumn). This
891 finding is consistent with Ma and Chen (2025), who showed that MHWs promote DCM development at the global
892 scale. In contrast, in winter or in vertically mixed upper ocean waters such as off SW WA, MHWs penetrate to depth,
893 eroding stratification and suppressing DCM. The level of stratification controls the thermocline depth, which we found

190

191

192

894 to be strongly correlated with DCM depth (Figs.10 and S5), and thereby governs both the vertical position of the DCM
895 and the MHW depth extent. Our results overall suggest that MHW-driven physical changes act to redistribute
896 chlorophyll vertically, with regional hydrography (through its influence on stratification) determining the extent of it,
897 consistent with hypothesis (4).

899 Regional differences in DO distributions during MHWs illustrate these complex interactions due to circulation and
900 stratification, and primary production. In NSW and TAS, MHWs generally decrease DO in the MLD (except summer
901 NSW), consistent with lower oxygen saturation level than during non-MHWs (Fig. S3), due to the temperature-
902 dependent decrease in oxygen solubility (negative DO tendency with temperature in Figs. S5c). However, below the
903 MLD, localized oxygen increases occur particularly in summer, near subsurface chlorophyll maxima (Figs.10, S5b.d).
904 These seasonal increases may reflect enhanced biological production during which oxygen is generated below the
905 MLD through photosynthesis, or ventilation associated with the strong East Australian Current (EAC) and its eddy-
906 driven intrusions (Malan et al., 2020). In addition to these biophysical drivers, regional wind patterns further modulate
907 the vertical structure of DO during spring in NSW. North-eastward winds in spring (Wood et al., 2016), favour
908 downwelling of warmer surface waters, contributing to the deeper vertical extent of MHWs and transporting oxygen
909 to subsurface layers.

910 DOX responses to MHW and their severity are less straightforward. Australia's surrounding waters exhibit distinct
911 oxygen regimes due to contrasting water masses, biogeochemical environments and seasonal variability. Low oxygen
912 regimes are usually present in tropical and subtropical regions (Paulmier and Ruiz-Pino, 2009; Davila et al., 2023)
913 such as QLD and SW WA, influenced by oxygen-poor water masses, while high oxygen regimes are found in
914 temperate regions (NSW, TAS), dominated by well-ventilated waters. During strong MHWs, low oxygen regimes
915 become more oxygenated in the MLD, potentially due to reduced upwelling of oxygen-poor waters under shallow
916 MLD. Despite lower nutrients from the subsurface, some regions still can experience enhanced primary production
917 due to light availability which in turn increases DOX in the MLD. Besides temperature's direct effect on oxygen
918 solubility, changes in DOX arise from complex interactions between circulation and stratification, and primary
919 productivity (Gruber, 2011; Gruber et al., 2021).

921 In QLD, DO responses to MHWs are linked to seasonal changes in stratification, mixing, and biological productivity.
922 During summer MHWs, strong near-surface stratification, reinforced by riverine freshening and wet-season rainfall,
923 creates a shallow MLD that traps heat and supports high biological activity. This results in elevated DO throughout
924 the upper water column, with oxygen saturation exceeding 100% in the MLD (Fig. S3), indicating that photosynthesis
925 more than compensates for the temperature-driven decline in oxygen solubility. This finding is in agreement with
926 hypothesis (2) that subsurface waters may experience enhanced oxygen concentrations associated with deeper
927 productivity. In contrast, autumn shows lower DO during MHWs compared to non-MHW periods, although
928 subsurface chlorophyll remains elevated. This reduction coincides with warmer and saltier conditions that decrease

199
929 oxygen solubility and combined with weaker stratification, facilitates the mixing of low-oxygen waters upward.
930 Enhanced respiration following the summer bloom may also deplete DO.

931 Regional differences in DOX distributions during MHWs illustrate these mechanisms. In NSW and TAS, MHWs
932 generally decrease DOX in the MLD (except spring NSW, spring and summer TAS), consistent with undersaturated
933 conditions (oxygen saturation below 100%; Fig. S2), due to the temperature-dependent decrease in oxygen solubility
934 (negative DOX tendency with temperature in Figs. S4a,c). However, below the MLD, localized oxygen increases
935 occur particularly in summer, near subsurface chlorophyll maxima (Figs.10, S4b,d). These seasonal increases may
936 reflect enhanced biological production during which oxygen is generated below the MLD through photosynthesis, or
937 ventilation associated with the strong East Australian Current (EAC) and its eddy-driven intrusions (Malan et al.,
938 2020). In addition to these biophysical drivers, regional wind patterns further modulate the vertical structure of DOX
939 during spring in NSW. North-eastward winds in spring (Wood et al., 2016), favour downwelling of warmer surface
940 waters, contributing to the deeper vertical extent of MHWs and transporting oxygen to subsurface layers.

941
942 In SW WA, well-mixed waters in the upper 40 m exhibited relatively uniform DO profiles, with enhanced DO in
943 summer and winter oxygenation during MHWs. For example, in summer, the weakened and offshore-displaced
944 Leeuwin Current combined with strong southerly winds (Feng et al., 2025) promotes strong ventilation and enhanced
945 mixing. During autumn, anomalously warm, fresh waters with reduced chlorophyll in the upper 20 m and reduced
946 DO, compared with non-MHW conditions, indicate the potential influence for intensified Leeuwin Current transport
947 to affect biogeochemical variables during advection-driven MHWs (Pearce and Feng, 2013). Overall, the study results
948 indicate that stratification and primary productivity jointly regulate oxygen variability, with regional hydrography
949 determining whether MHWs enhance or suppress oxygenation across the water column.

950 In QLD, DOX responses to MHWs are linked to seasonal changes in stratification, mixing, and biological productivity.
951 During summer MHWs, strong near-surface stratification, reinforced by riverine freshening and wet-season rainfall,
952 creates a shallow MLD that traps heat and supports high biological activity. This results in elevated DOX throughout
953 the upper water column, with oxygen saturation exceeding 100% in the MLD (Fig. S2), indicating that photosynthesis
954 more than compensates for the temperature-driven decline in oxygen solubility. In contrast, autumn shows lower DOX
955 during MHWs compared to non-MHW periods, although subsurface chlorophyll remains elevated. This reduction
956 coincides with warmer and saltier conditions that decrease oxygen solubility and combined with weaker stratification,
957 facilitates the mixing of low-oxygen waters upward. Enhanced respiration following the summer bloom may also
958 deplete DOX.

959
960 While this study provides a comprehensive analysis of subsurface thermal and biogeochemical structure associated
961 with surface MHWs, several limitations related to sampling density should be acknowledged. Despite the availability
962 of 16 years of glider observations, sampling remains uneven across regions, depths and seasons, which constrains the
963 robustness of some composite profiles. In particular, subsurface properties during spring MHWs are not robustly
964 characterised in some regions due to the small number of captured events. For example, TAS in spring are based on

203

204

965 only two MHW events, limiting confidence in the seasonal mean of these profiles. Similarly, in QLD, the number of
966 MHW profiles during autumn exceeds that of non-MHW profiles, which may not give a true representation of the
967 seasonal mean.

968 In SW WA, well-mixed waters in the upper 40 m exhibited relatively uniform DOX profiles, with enhanced DOX in
969 summer and winter oxygenation during MHWs. For example, in summer, the weakened and offshore-displaced
970 Leeuwin Current combined with strong southerly winds (Feng et al., 2025) promotes strong ventilation and enhanced
971 mixing. During autumn, anomalously warm, fresh waters with reduced chlorophyll in the upper 20 m and reduced
972 DOX, compared with non-MHW conditions, indicate the potential influence for intensified Leeuwin Current transport
973 to affect biogeochemical variables during advection-driven MHWs (Pearce and Feng, 2013). Overall, the study results
974 indicate that stratification and primary productivity jointly regulate oxygen variability, with regional hydrography
975 determining whether MHWs enhance or suppress oxygenation across the water column.

976

977 Additional limitations arise from combining surface MHW detection based on daily, night-time, gap-filled satellite
978 data with sub-daily in situ glider observations, which may bring inconsistencies between both surface and subsurface
979 signals. Furthermore, the available dataset is insufficient to assess the influence of large-scale climate modes on the
980 subsurface structure of surface MHWs, and lack some biological parameters (e.g. nutrient concentrations) which
981 restricts the interpretation of DO and DCM. Addressing these limitations will require high-resolution observations
982 across all seasons and coordinated modelling efforts to develop robust subsurface climatologies.

205

206

207

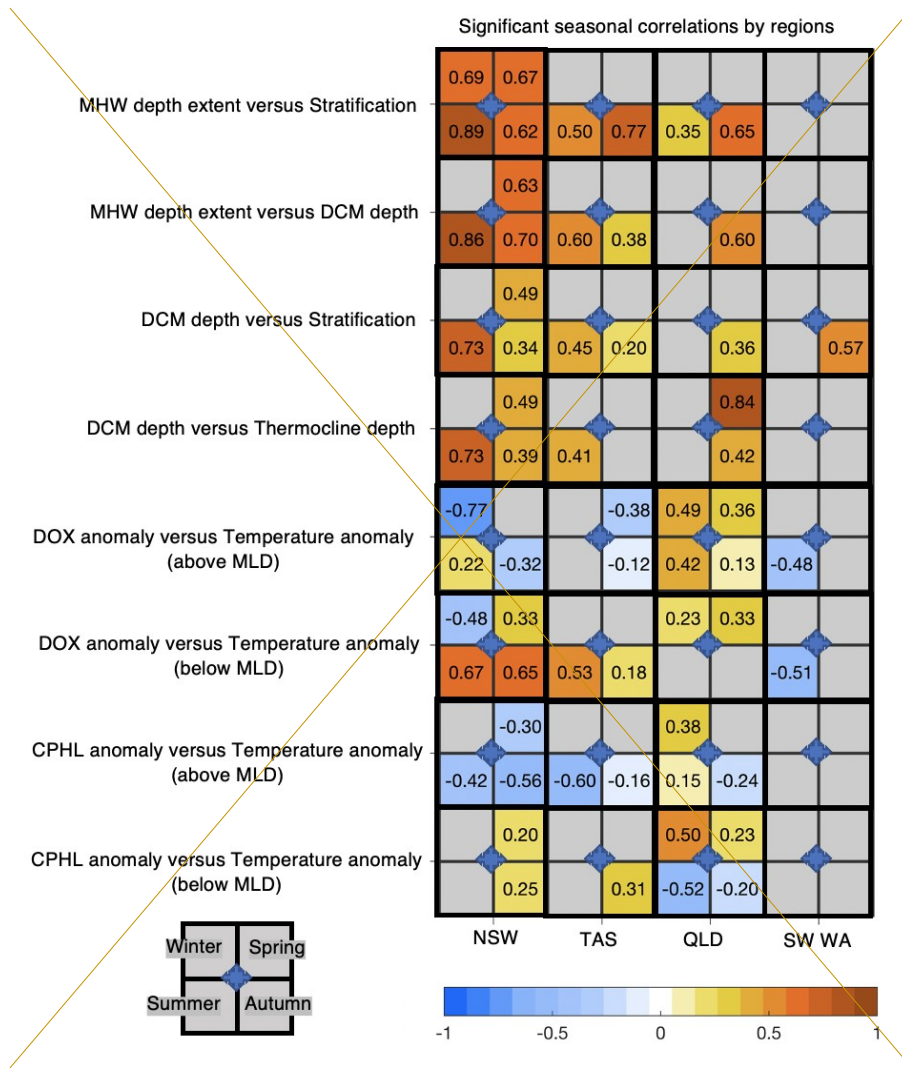


Figure 10. Synthesis figure of seasonal correlations between key physical-biogeochemical variables during MHWs across four regions (NSW, TAS, QLD, SW WA). Rows correspond to variable pairs: (1) MHW depth extent versus stratification; (2) MHW depth extent versus deep DCM depth, (3) DCM depth versus stratification, (4) DCM depth versus thermocline depth, (5) dissolved oxygen anomalies (DOX) versus temperature anomalies (above the MLD), (6) dissolved oxygen anomalies (DOX) versus temperature anomalies (below the MLD); (7) chlorophyll anomalies versus temperature anomalies (in the MLD); and (8) chlorophyll anomalies versus temperature anomalies (below the MLD). Columns correspond to regions. Each cell is subdivided into four seasonal quadrants, colored by the Pearson correlation coefficient (r) values with values indicated within each quadrant.

993 **5. Conclusions**

994 This study shows that the impacts of MHWs on dissolved oxygen and chlorophyll along the Australian continental
 995 shelf depend strongly on regional hydrography, seasonal stratification, and, to some extent, event severity. Taken

213

214

996 together, our results show that surface-only perspectives underestimate the biogeochemical and potential ecological
997 impacts of MHWs. Subsurface glider observations revealed that MHWs can simultaneously suppress surface
998 productivity while intensifying subsurface production, with consequences for oxygen levels and food-web dynamics,
999 depending on regional hydrography and stratification. Stratification, which appears consistently enhanced during
1000 summer MHWs, emerges as a useful proxy for the vertical extent of surface MHWs and on the DCM. These findings
1001 underscore the importance of accounting for region-specific monitoring to manage ecological consequences of
1002 MHWs.

1003

1004 The interaction between physical processes, such as seasonal circulation, stratification and biological feedback,
1005 including deep chlorophyll maxima formation and oxygen production, highlights the complex biogeochemical
1006 responses to MHWs. By leveraging up to 16 years of glider observations, this work demonstrates the importance of
1007 sustained subsurface monitoring and coupled physical–biogeochemical approaches to better predict ecosystem
1008 vulnerability. Future research is needed to transform sparse and high-frequency sampling of continental shelf waters
1009 to develop coastal climatologies appropriate for assessing subsurface ~~MHW~~marine heatwave impacts. Long-term
1010 measurements are key to improving our understanding of MHWs' vertical structure, drivers, and ecological
1011 consequences and, in combination with shelf modelling, can provide a holistic view of how they affect variability and
1012 extremes in our coastal and shelf systems. These efforts are critical for managing the impacts of MHWs on marine
1013 ecosystems under a warming climate.

1014

1015 **Data availability:** The glider data is publicly available through the Australian Ocean Data Network (AODN) Portal
1016 at: <https://portal.aodn.org.au/search?uuid=c317b0fe-02e8-4ff9-96c9-563fd58e82ac> and
1017 <https://thredds.aodn.org.au/thredds/catalog/IMOS/ANFOG/catalog.html>.

1018 The NOAA CoralTemp v3.1 SST product is available at: <https://coralreefwatch.noaa.gov/product/5km/index.php>.

1019 The IMOS OceanCurrent delayed-mode, gridded (adjusted) sea level anomaly product and surface geostrophic
1020 velocity is available from 1993–2020 at: [https://thredds.aodn.org.au/thredds/catalog/IMOS/OceanCurrent/GSLA/](https://thredds.aodn.org.au/thredds/catalog/IMOS/OceanCurrent/GSLA/DM/catalog.html)
1021 [DM/catalog.html](https://thredds.aodn.org.au/thredds/catalog/IMOS/OceanCurrent/GSLA/DM/catalog.html), while the near-real-time data is available at:

1022 <https://thredds.aodn.org.au/thredds/catalog/IMOS/OceanCurrent/GSLA/NRT/catalog.html>.

1023

215

216

217

218

219

1024 | **Code availability:** Processed glider data and code can be accessed at [https://github.com/GlidersMHWs/Subsurface-](https://github.com/GlidersMHWs/Subsurface-biogeochemical-marine-heatwaves-on-the-Australian-continental-shelf/tree/main)
1025 | [biogeochemical-marine-heatwaves-on-the-Australian-continental-shelf/tree/main](https://github.com/GlidersMHWs/Subsurface-biogeochemical-marine-heatwaves-on-the-Australian-continental-shelf/tree/main)

1026 | **Code availability:** The code will be available at the time of publication on Github.

1027 | **Author contributions:** DM lead the project in assigning analysis and writing. JA and RLG assisted with data
1028 | reprocessing. AS designed and supervised the project. All authors contributed to the analyses, discussions, writing
1029 | and proofreading.

1030 | **Competing interests:** The authors declare that they have no conflict of interest.

1031 | **Acknowledgments:** We would like to acknowledge CLIVAR (Climate and Ocean – Variability, Predictability and
1032 | Change) 2023 Marine heatwave summer school, through which this project started. We also thank everyone who was
1033 | involved in the glider deployment, piloting, and processing, through the IMOS Ocean Gliders Facility led by Prof.
1034 | Charitha Pattiaratchi, as well as the IMOS Event Based Sampling national committee. All glider data were sourced
1035 | from Australia’s Integrated Marine Observing System (IMOS) – IMOS is enabled by the National Collaborative
1036 | Research Infrastructure Strategy (NCRIS). It is operated by a consortium of institutions as an unincorporated joint
1037 | venture, with the University of Tasmania as Lead Agent.

1038 | **Financial support:**

1039

1040 | FEKG. acknowledges funding from Canada’s C150 Research Program (Grant No. 50296) and Schmidt Sciences,
1041 | LLC.

1042

1043 | **References**

1044 | Amaya, D. J., Miller, A. J., Xie, S.-P., and Kosaka, Y.: Physical drivers of the summer 2019 North Pacific marine
1045 | heatwave, *Nat. Commun.*, 11(1), 1903, doi:10.1038/s41467-020-15820-w, 2020

1046 | Benthuisen, J., Feng, M., and Zhong L.: Spatial patterns of warming off Western Australia during the 2011 Ningaloo
1047 | Niño: Quantifying impacts of remote and local forcing, *Cont. Shelf Res.*, 91, 232-246,
1048 | doi:10.1016/j.csr.2014.09.014, 2014.

1049 | Benthuisen, J. A., Tonin, H., Brinkman, R., Herzfeld, M., and Steinberg, C.: Intrusive upwelling in the Central Great
1050 | Barrier Reef. *J. of Geophys. Res.: Oceans*, 121(11), pp.8395-8416, doi:10.1002/2016JC012294, 2016.

1051 | Benthuisen, J. A., Oliver, E. C. J., Feng, M., and Marshall, A. G.: Extreme marine warming across tropical Australia
1052 | during austral summer 2015–2016, *J. Geophys. Res.: Oceans*, 123(2), 1301-1326, doi:10.1002/2017JC013326,
1053 | 2018.

1054 | Benthuisen, J. A., Steinberg, C., Spillman, C. M., and Smith, G. A.: Oceanographic drivers of bleaching in the GBR:
1055 | from observations to prediction. Volume 4: Observations and predictions of marine heatwaves. Report to the

220

221

222

1056 National Environmental Science Program. Reef and Rainforest Research Centre Limited, Cairns (47pp.). Available
1057 at: <https://nesptropical.edu.au/index.php/round-4-projects/project-4-2/>, 2021.

1058 Benthuisen, J. A., Emslie, M. J., Currey-Randall, L. M., Cheal, A. J. and Heupel, M. R.: Oceanographic influences
1059 on reef fish assemblages along the Great Barrier Reef, *Prog. Oceanogr.*, 208, p.102901,
1060 doi:10.1016/j.pocean.2022.102901, 2022.

1061 Benthuisen, J. A., Pattiaratchi, C., Spillman, C. M., Govekar, P., Beggs, H., Bastos de Oliveira, H., Chandrapavan,
1062 A., Feng, M., Hobday, A. J., Holbrook, N. J., Jaime, F. R. A., and Schaeffer, A.: Observing marine heatwaves
1063 using ocean gliders to address ecosystem challenges through a coordinated national program. In *Frontiers in Ocean*
1064 *Observing*. E.S. Kappel, V. Cullen, I.C.A. da Silveira, G. Coward, C. Edwards, P. Heimbach, T. Morris, H. Pillar,
1065 M. Roughan, and J. Wilkin, eds, *Oceanogr.* 38(Supplement 1), doi:10.5670/oceanog.2025e101, 2025.

1066 Berkelmans, R., & Oliver, J. K.: Large-scale bleaching of corals on the Great Barrier Reef. *Coral reefs*, 18(1), 55-60,
1067 doi:10.1007/s003380050154, 1999.

1068 Blondeau-Patissier, D., Gower, J. F. R., Dekker, A. G., Phinn, S. R., and Brando, V. E.: A review of ocean color
1069 remote sensing methods and statistical techniques for the detection, mapping and analysis of phytoplankton blooms
1070 in coastal and open oceans, *Prog. Oceanogr.*, 123, 123–144, doi:10.1016/j.pocean.2013.12.008, 2014.

1071 Brooke, B., Creasey, J., and Sexton, M.: Broad-scale geomorphology and benthic habitats of the Perth coastal plain
1072 and Rottneest Shelf, Western Australia, identified in a merged topographic and bathymetric digital relief model,
1073 *Intern. J. Rem. Sens.*, 31(23), 6223–6237, doi: 10.1080/01431160903403052, 2010.

1074 Capotondi, A., Rodrigues, R. R., Sen Gupta, A., Benthuisen, J. A., Deser, C., Frölicher, T. L., Lovenduski, N. S.,
1075 Amaya, D. J., Le Grix, N., Xu, T., and Hermes, J.: A global overview of marine heatwaves in a changing climate,
1076 *Commun. Earth Environ.*, 5, 701, doi:10.1038/s43247-024-01806-9, 2024.

1077 Cavole, L. M., Demko, A. M., Diner, R. E., Giddings, A., Koester, I., Pagniello, C. M., ... and Franks, P. J.: Biological
1078 impacts of the 2013–2015 warm-water anomaly in the Northeast Pacific: winners, losers, and the future, *Oceanogr.*,
1079 29(2), 273-285. doi:10.5670/oceanog.2016.32, 2016.

1080 Chen, M., Pattiaratchi, C. B., Ghadouani, A., and Hanson, C.: Seasonal and inter-annual variability of water column
1081 properties along the Rottneest continental shelf, south-west Australia, *Ocean Sci.*, 15, 333–348, doi:10.5194/os-15-
1082 333-2019, 2019.

1083 Chen, M., Pattiaratchi, C. B., Ghadouani, A. and Hanson C.: Influence of storm events on chlorophyll distribution
1084 along the oligotrophic continental shelf off south-western Australia, *Front. Mar. Sci.*, 7, 287,
1085 doi:10.3389/fmars.2020.00287, 2020.

1086 Chen, Q., Li, D., Feng, J., Zhao, L., Qi, J., and Yin, B.: Understanding the compound marine heatwave and low-
1087 chlorophyll extremes in the western Pacific Ocean, *Front. Mar. Sci.*, 10, 1303663,
1088 doi:10.3389/fmars.2023.1303663, 2023.

1089 Chiswell, S. M.: Tasman Sea high- and low- chlorophyll events, their links to marine heat waves, cool spells, and
1090 global teleconnections, *New Zealand J. Mar. Fresh. Res.*, 57(4), 550–567, doi:10.1080/00288330.2022.2076702,
1091 2023.

- 1092 Davila, X., Olsen, A., Lauvset, S. K., McDonagh, E. L., Brakstad, A., and Gebbie, G.: On the origins of open ocean
1093 oxygen minimum zones, *J. Geophys. Res.: Oceans*, 128(8), e2023JC019677, doi:10.1029/2023JC019677, 2023.
- 1094 Davies, K. T.: Using passive acoustic monitoring from gliders for near realtime detection and dynamic management
1095 of North Atlantic right whales (*Eubalaena glacialis*) in the Laurentian Channel Dynamic Shipping Zones, 2021.
- 1096 Eakins, B. W., and Sharman, G. F.: ~~(2010)~~. Volumes of the World's Oceans from ETOPO1. NOAA National
1097 Geophysical Data Center, Boulder, CO, 7(1), 2010.
- 1098 [Elzahaby, Y., and Schaeffer, A.: Observational insight into the subsurface anomalies of marine heatwaves, *Frontiers*
1099 *in Marine Science*, 6, doi:10.3389/fmars.2019.00745, 2019.](#)
- 1100 Feng, M., McPhaden, M. J., Xie, S.-P., and Hafner, J.: La Niña forces unprecedented Leeuwin Current warming in
1101 2011, *Sci. Rep.*, 3(1), 1277, doi:10.1038/srep01277, 2013.
- 1102 Feng, M., Benthuyesen, J., Zhang, N., and Slawinski, D.: Freshening anomalies in the Indonesian throughflow and
1103 impacts on the Leeuwin Current during 2010–2011, *Geophys. Res. Lett.*, 42(20), 8555-8562,
1104 doi:10.1002/2015GL065848, 2015.
- 1105 Feng, M., Caputi, N., Chandrapavan, A., Chen, M., Hart, A., and Kangas, M.: Multi-year marine cold-spells off the
1106 west coast of Australia and effects on fisheries, *J. Mar. Sys.*, 214, 103473, doi:10.1016/j.jmarsys.2020.103473,
1107 2021.
- 1108 Feng, M., Bui, T., and Benthuyesen, J. A.: Seasonal climatology of the Leeuwin Current–Capes Current system off
1109 southwest Australia from long–term moored observations, *J. Geophys. Res.: Oceans*, 130(5), e2025JC022662,
1110 doi:10.1029/2025JC022662, 2025.
- 1111 Frölicher, T. L., Fischer, E. M. and Gruber, N.: Marine heatwaves under global warming, *Nature*, 560, 360–364,
1112 doi:10.1038/S31586-018-0383-9, 2018.
- 1113 Garcia, H. E., & Gordon, L. I.: Oxygen solubility in seawater: Better fitting equations. *Limnology and*
1114 *oceanography*, 37(6), 1307-1312, doi:10.4319/lo.1992.37.6.1307, 1992.
- 1115 Gomes, D. G., Ruzicka, J. J., Crozier, L. G., Huff, D. D., Brodeur, R. D., and Stewart, J. D.: Marine heatwaves disrupt
1116 ecosystem structure and function via altered food webs and energy flux. *Nat. Commun.*, 15(1), 1988.
1117 doi:10.1038/s41467-024-46263-2, 2024.
- 1118 Great Barrier Reef Marine Park Authority, Australian Institute of Marine Science, and CSIRO.: Reef Snapshot:
1119 Summer 2024–25, Reef Authority, Townsville, Available at: <https://hdl.handle.net/11017/4116>, 2025.
- 1120 Gregory, C. H., Holbrook, N. J., Marshall, A. G., and Spillman, C. M.: Atmospheric drivers of Tasman Sea marine
1121 heatwaves, *J. Climate*, 36(15), 5197-5214, doi:10.1175/JCLI-D-22-0538.1, 2023.
- 1122 Gruber, N.: Warming up, turning sour, losing breath: ocean biogeochemistry under global change, *Phil. Trans. R. Soc.*
1123 *A.*, 3691980, doi:10.1098/rsta.2011.0003, 2011.
- 1124 Gruber, N., Boyd, P. W., Frölicher, T. L., and Vogt, M.: Biogeochemical extremes and compound events in the ocean,
1125 *Nature*, 600, 395–407, doi:10.1038/s41586-021-03981-7, 2021.

- 1126 Hanson, C. E., Pattiaratchi, C. B., and Waite, A. M.: Sporadic upwelling on a downwelling coast: phytoplankton
 1127 responses to spatially variable nutrient dynamics off the Gascoyne region of Western Australia, *Cont. Shelf Res.*,
 1128 25(12-13), 1561-1582, doi:10.1016/j.csr.2005.04.003, 2005.
- 1129 Hayashida, H., Matear, R. J., and Strutton, P. G.: Background nutrient concentration determines phytoplankton bloom
 1130 response to marine heatwaves, *Glob. Change Bio.*, 26(9), 4800-4811, doi:10.1111/gcb.15255, 2020.
- 1131 Hill, K. L., Rintoul, S. R., Coleman, R., and Ridgway, K. R.: Wind forced low frequency variability of the East
 1132 Australia Current, *Geophys. Res. Lett.*, 35(8), doi:10.1029/2007GL032912, 2008.
- 1133 Hobday, A. J., & Pecl, G. T.: Identification of global marine hotspots: sentinels for change and vanguards for
 1134 adaptation action. *Reviews in Fish Biology and Fisheries*, 24(2), 415-425, doi:10.1007/s11160-013-9326-6, 2014.
- 1135 Hobday, A. J., Alexander, L. V., Perkins, S. E., Smale, D. A., Straub, S. C., Oliver, E. C. J., Benthuyesen, J. A.,
 1136 Burrows, M. T., Donat, M. G., Feng, M., and Holbrook, N. J.: A hierarchical approach to defining marine
 1137 heatwaves, *Prog. Oceanogr.*, 141, 227-238, doi:10.1016/j.pocean.2015.12.014, 2016.
- 1138 Hobday, A. J., Oliver, E. C., Sen Gupta, A., Benthuyesen, J. A., Burrows, M. T., Donat, M. G., ... and Smale, D. A.:
 1139 Categorizing and naming marine heatwaves, *Oceanogr.*, 31(2), 162-173, doi:10.5670/oceanog.2018.205, 2018.
- 1140 Holbrook, N. J., and Bindoff, N. L.: Interannual and decadal temperature variability in the southwest Pacific Ocean
 1141 between 1955 and 1988, *J. Clim.*, 10(5), 1035-1049. doi:10.1175/1520-0442(1997)010<1035:IADTVI>2.0.CO;2,
 1142 1997.
- 1143 Holbrook, N. J., Hernaman, V., Koshiha, S., Lako, J., Kajtar, J. B., Amosa, P., and Singh, A.: Impacts of marine
 1144 heatwaves on tropical western and central Pacific Island nations and their communities, *Global and Planetary
 1145 Change*, 208, 103680, doi.org/10.1016/j.gloplacha.2021.103680, 2022.
- 1146 Huang, Z., Feng, M., Dalton, S. J., and Carroll, A. G.: Marine heatwaves in the Great Barrier Reef and Coral Sea:
 1147 their mechanisms and impacts on shallow and mesophotic coral ecosystems, *Sci. Total Env.*, 908, 168063,
 1148 doi:10.1016/j.scitotenv.2023.168063, 2024.
- 1149 IMOS 2025, "OceanCurrent - Gridded sea level anomaly - Delayed mode - DM02", [https://catalogue-](https://catalogue-imos.aodn.org.au/geonetwork/srv/eng/catalog.search#/metadata/da30c0b8-4978-4a26-915e-b80c88bb4510)
 1150 [imos.aodn.org.au/geonetwork/srv/eng/catalog.search#/metadata/da30c0b8-4978-4a26-915e-b80c88bb4510](https://catalogue-imos.aodn.org.au/geonetwork/srv/eng/catalog.search#/metadata/da30c0b8-4978-4a26-915e-b80c88bb4510),
 1151 accessed August-2025.
- 1152 Kwiatkowski, L., Torres, O., Bopp, L., Aumont, O., Chamberlain, M., Christian, J. R., ... & Ziehn, T.: Twenty-first
 1153 century ocean warming, acidification, deoxygenation, and upper-ocean nutrient and primary production decline
 1154 from CMIP6 model projections. *Biogeosciences*, 17(13), 3439-3470, doi:10.5194/bg-17-3439-2020, 2020.
- 1155 Lachkar, Z., Lévy, M., and Smith, K. S.: Strong intensification of the Arabian Sea oxygen minimum zone in response
 1156 to Arabian Gulf warming. *Geophys. Res. Lett.*, 46(10), 5420-5429, doi:10.1029/2018GL081631, 2019.
- 1157 Laufkötter, C., Zscheischler, J., and Frölicher, T. L.: High-impact marine heatwaves attributable to human-induced
 1158 global warming, *Science*, 369(6511), 1621-1625. doi:10.1126/science.aba0690, 2020.
- 1159 Le Gendre, R., Varillon, D., Fiat, S., Hocdé, R., de Ramon N'Yeurt, A., Andréfouët, S., ... & Menkes, C.: ReefTEMPS:
 1160 the Pacific Islands coastal temperature network. *Earth System Science Data*, 17(10), 5277-5301,
 1161 doi:10.5194/essd-17-5277-202510.5194/essd-17-5277-2025, 2025.

- 1162 Le Grix, N., Zscheischler, J., Laufkötter, C., Rousseaux, C. S., and Frölicher, T. L.: Compound high temperature and
 1163 low chlorophyll extremes in the ocean over the satellite period, *Biogeosci. Discussions*, 2020, 1-26.
 1164 doi:10.5194/bg-18-2119-2021, 2020.
- 1165 Ma, X. and Chen, G.: Marine heatwaves are shaping the vertical structure of phytoplankton in the global ocean.
 1166 *Commun. Earth Environ.*, 6, 715, doi:10.1038/S33247-025-02718-y, 2025.
- 1167 Malan, N., Archer, M., Roughan, M., Cetina-Heredia, P., Hemming, M., Rocha, C., ... and Queiroz, E.: Eddy-driven
 1168 cross-shelf transport in the East Australian Current separation zone, *J. Geophys. Res.: Oceans*, 125(2),
 1169 e2019JC015613, doi: 10.1029/2019JC015613, 2020.
- 1170 Malan, N., Sen Gupta, A., Schaeffer, A., Zhang, S., Doblin, M. A., Pilo, G. S., ... and Spillman, C. M.: Lifting the lid
 1171 on marine heatwaves, *Prog. Oceanogr.*, 103539. doi:10.1016/j.pocean.2025.103539, 2025.
- 1172 Marre, J. B., Thebaud, O., Pascoe, S., Jennings, S., Boncoeur, J., and Coglán, L.: The use of ecosystem services
 1173 valuation in Australian coastal zone management, *Marine Policy*, 56, 117-124, doi:10.1016/j.marpol.2015.02.011,
 1174 2015.
- 1175 Meier, H. M., Väli, G., Naumann, M., Eilola, K., and Frauen, C.: Recently accelerated oxygen consumption rates
 1176 amplify deoxygenation in the Baltic Sea, *J. Geophys. Res.: Oceans*, 123(5), 3227-3240,
 1177 doi:10.1029/2017JC013686, 2018.
- 1178 Noh, K. M., Lim, H. G., and Kug, J. S.: Global chlorophyll responses to marine heatwaves in satellite ocean color.
 1179 *Environ. Res. Lett.*, 17(6), 064034, doi:10.1088/1748-9326/ac70ec, 2022.
- 1180 Oliver, E. C., Benthuisen, J. A., Bindoff, N. L., Hobday, A. J., Holbrook, N. J., Mundy, C. N., and Perkins-Kirkpatrick,
 1181 S. E.: The unprecedented 2015/16 Tasman Sea marine heatwave, *Nat. Commun.*, 8(1), 16101,
 1182 doi:10.1038/ncomms16101, 2017.
- 1183 Oliver, E. C., Benthuisen, J. A., Darmaraki, S., Donat, M. G., Hobday, A. J., Holbrook, N. J., ... and Sen Gupta, A.:
 1184 Marine heatwaves, *Ann. Rev. Mar. Sci.*, 13(1), 313-342, doi:10.1146/annurev-marine-032720-095144, 2021.
- 1185 Pattiaratchi, C., Hollings, B., Woo, M., and Welhena, T.: Dense shelf water formation along the south-west Australian
 1186 inner shelf, *Geophys. Res. Lett.*, 38, L10609, doi:10.1029/2011GL046816, 2011.
- 1187 Pattiaratchi, C., Woo, L. M., Thomson, P. G., Hong, K. K., and Stanley, D.: Ocean glider observations around
 1188 Australia. *Oceanogr.*, 30(2), 90-91, doi:10.5670/oceanog.2017.226, 2017.
- 1189 Paulmier, A. and Ruiz-Pino, D.: Oxygen minimum zones (OMZs) in the modern ocean.: *Prog. Oceanogr.*, 80(3-4),
 1190 113-128, doi:10.1016/j.pocean.2008.08.001, 2009.
- 1191 Pearce, A., Lenanton, R., Jackson, G., Moore, J., Feng, M., and Gaughan, D.: The “marine heat wave” off Western
 1192 Australia during the summer of 2010/11, Fisheries Research Report No. 222, Department of Fisheries, Western
 1193 Australia. 40pp., Available at: https://www.fish.wa.gov.au/documents/research_reports/fr222.pdf, 2011.
- 1194 Pearce, A. F. and Feng, M.: The rise and fall of the “marine heat wave” off Western Australia during the summer of
 1195 2010/2011, *J. Mar. Sys.*, 111, 139-156, doi:10.1016/j.jmarsys.2012.10.009, 2013.
- 1196 Richardson, A. J., Savage, J., Coman, F., Davies, C., Eriksen, R., McEnulty, F., Slotwinski, A., Tonks, M., Uribe-
 1197 Palomino, J.: The impact on zooplankton of the 2011 heatwave off Western Australia. In Richardson, A. J.,
 240

1198 Eriksen, R., Moltmann, T., Hodgson-Johnston, I., Wallis, J. R. (Eds). State and trends of Australia's ocean Report,
1199 doi:10.26198/5e16adc449e87, 2020.

1200 Ridgway, K. R.: Long-term trend and decadal variability of the southward penetration of the East Australian Current,
1201 *Geophys. Res. Lett.*, 34(13), doi:10.1029/2007GL030393, 2007.

1202 Ridgway, K. R., Benthuysen, J. A., and Steinberg, C.: Closing the gap between the Coral Sea and the equator: Direct
1203 observations of the north Australian western boundary currents, *J. Geophys. Res.: Oceans*, 123(12), 9212-9231,
1204 doi:10.1029/2018JC014269, 2018.

1205 Ridgway, K. R. and Ling, S. D.: Three decades of variability and warming of nearshore waters around Tasmania,
1206 *Prog. Oceanogr.*, 215, 103046, doi:10.1016/j.pocean.2023.103046, 2023.

1207 Roberts, S. D., Van Ruth, P. D., Wilkinson, C., Bastianello, S. S., & Bansemer, M. S.: Marine heatwave, harmful
1208 algae blooms and an extensive fish kill event during 2013 in South Australia. *Frontiers in Marine Science*, 6, 610,
1209 doi:10.3389/fmars.2019.00610, 2019.

1210 Rose, T. H., Smale, D. A., and Botting, G.: The 2011 marine heat wave in Cockburn Sound, southwest Australia.
1211 *Ocean Sci.*, 8(4), 545-550, doi:10.5194/os-8-545-2012, 2012.

1212 Rudnick, D. L.: Ocean research enabled by underwater gliders, *Ann. Rev. Mar. Sci.*, 8(1), 519-541,
1213 doi:10.1146/annurev-marine-122414-033913, 2016.

1214 Safonova, K., Meier, H. M., and Gröger, M.: Summer heatwaves on the Baltic Sea seabed contribute to oxygen
1215 deficiency in shallow areas, *Comm. Earth Environ.*, 5(1), 106, doi:10.1038/s43247-024-01268-z, 2024.

1216 Sampaio, E., Santos, C., Rosa, I. C., Ferreira, V., Pörtner, H.-O., Duarte, C. M., Levin, L. A., and Rosa, R.: Impacts
1217 of hypoxic events surpass those of future ocean warming and acidification, *Nat. Ecol. Evol.*, 5(3), 311-321,
1218 doi:10.1038/s41559-020-01370-3, 2021.

1219 Schaeffer, A., Roughan, M., & Wood, J. E.: Observed bottom boundary layer transport and uplift on the continental
1220 shelf adjacent to a western boundary current. *Journal of Geophysical Research: Oceans*, 119(8), 4922-4939,
1221 doi:10.1002/2013JC009735, 2014.

1222 Schaeffer, A., Roughan, M., Jones, E. M., and White, D.: Physical and biogeochemical spatial scales of variability in
1223 the East Australian Current separation from shelf glider measurements, *Biogeosciences*, 13, 1967-1975,
1224 doi:10.5194/bg-13-1967-2016, 2016a.

1225 Schaeffer, A., Roughan, M., Austin, T., Everett, J. D., Griffin, D., Hollings, B., ... and White, D.: Mean hydrography
1226 on the continental shelf from 26 repeat glider deployments along southeastern Australia, *Sci. Data*, 3(1), 1-12,
1227 doi:10.1038/sdata.2016.70, 2016b.

1228 Schaeffer, A., and Roughan, M.: Subsurface intensification of marine heatwaves off southeastern Australia: The role
1229 of stratification and local winds, *Geophys. Res. Lett.*, 44(10), 5025-5033, doi:10.1002/2017GL073714, 2017.

1230 Schaeffer, A., Sen Gupta, A., and Roughan, M.: Seasonal stratification and complex local dynamics control the sub-
1231 surface structure of marine heatwaves in Eastern Australian coastal waters, *Commun. Earth Environ.*, 4(1), 304,
1232 doi: 10.1038/s43247-023-00966-4, 2023.

1233 Schiller, A., Ridgway, K. R., Steinberg, C. R., and Oke, P. R.: Dynamics of three anomalous SST events in the Coral
1234 Sea, *Geophys. Res. Lett.*, 36(6), doi:10.1029/2008GL036997, 2009.

1235 Schroeder, T., Devlin, M. J., Brando, V. E., Dekker, A. G., Brodie, J. E., Clementson, L. A., & McKinna, L.: Inter-
1236 annual variability of wet season freshwater plume extent into the Great Barrier Reef lagoon based on satellite
1237 coastal ocean colour observations. *Marine Pollution Bulletin*, 65(4–9), 210–223,
1238 doi:10.1016/j.marpolbul.2012.02.022, 2012.

1239 Sen Gupta, A., Thomsen, M., Benthuisen, J. A., Hobday, A. J., Oliver, E., Alexander, L. V., ... and Smale, D. A.:
1240 Drivers and impacts of the most extreme marine heatwave events, *Sci. Rep.*, 10, doi:10.1038/S31598-020-75445-3,
1241 2020.

1242 Siefert, R. L. and Plattner, G.-K.: The role of coastal zones in global biogeochemical cycles, *Eos Trans. AGU*, 85(45),
1243 470-470, doi:10.1029/2004EO450005, 2004.

1244 Skirving, W., Marsh, B., De La Cour, J., Liu, G., Harris, A., Maturi, E., ... and Eakin, C. M.: CoralTemp and the Coral
1245 Reef Watch coral bleaching heat stress product suite version 3.1, *Rem. Sens.*, 12(23), 3856,
1246 doi:10.3390/rs12233856, 2020.

1247 Smith, K. E., Burrows, M. T., Hobday, A. J., King, N. G., Moore, P. J., Sen Gupta, A., Moore, P. J., Thomsen, M.,
1248 Wernberg, T., and Smale, D. A.: Socioeconomic impacts of marine heatwaves: Global issues and opportunities,
1249 *Science*, 374, eabj3593, doi:10.1126/science.abj3593, 2021.

1250 Smith, K. E., Burrows, M. T., Hobday, A. J., King, N. G., Moore, P. J., Sen Gupta, A., Moore, P. J., Thomsen, M.,
1251 Wernberg, T., and Smale, D. A.: Biological impacts of marine heatwaves, *Ann. Rev. Mar. Sci.*, 15 (1), 119-145,
1252 doi:10.1146/annurev-marine-032122-121437, 2023.

1253 [Stammer, D., Wunsch, C., & Ueyoshi, K.: Temporal changes in ocean eddy transports. *Journal of Physical*
1254 *Oceanography*, 36\(3\), 543-550, doi:10.1175/JPO2858.1, 2006.](#)

1255 Tassone, S. J., Besterman, A. F., Buelo, C. D., Walter, J. A., and Pace, M. L.: Co-occurrence of aquatic heatwaves
1256 with atmospheric heatwaves, low dissolved oxygen, and low pH events in estuarine ecosystems, *Estuar. Coasts*,
1257 45(3), 707-720, doi:10.1007/s12237-021-01009-x, 2022.

1258 Testor, P., de Young, B., Rudnick, D. L., Glenn, S., Hayes, D., Lee, C. M., Pattiaratchi, C., Hill, K., Heslop, E., Turpin,
1259 V., Alenius, P., ... and Wilson, D.: OceanGliders: a component of the integrated GOOS, *Front. Mar. Sci.*, 6, 422,
1260 doi:10.3389/fmars.2019.00422, 2019.

1261 Walsh, S. J.: Commercial fishing practices on offshore juvenile flatfish nursery grounds on the Grand Banks of
1262 Newfoundland, *Netherlands J. Sea Res.*, 27(3-4), 423-432, doi:10.1016/0077-7579(91)90043-Z, 1991.

1263 Wang, Y., Holbrook, N. J., and Kajtar, J. B.: Predictability of marine heatwaves off Western Australia using a linear
1264 inverse model, *J. Clim.*, 36(18), 6177-6193, doi:10.1175/JCLI-D-22-0692.1, 2023.

1265 Weller, E., Holliday, D., Feng, M., Beckley, L., and Thompson, P.: A continental shelf scale examination of the
1266 Leeuwin Current off Western Australia during the austral autumn–winter, *Cont. Shelf Res.*, 31(17), 1858-1868,
1267 doi:10.1016/j.csr.2011.08.008, 2011.

253

254

1268 Wolanski, E. and Kingsford, M. (Eds.): Oceanographic processes of coral reefs: Physical and biological links in the
1269 Great Barrier Reef (Second edition), CRC Press, Boca Raton, doi:10.1201/9781003320425, 2024.

1270 Woo, M. and Pattiaratchi, C.: Hydrography and water masses off the western Australian coast, Deep Sea Research
1271 Part I: Oceanographic Research Papers, 55(9), 1090-1104, doi:10.1016/j.dsr.2008.05.005, 2008.

1272 Woo, L. M. and Gourcuff, C.: Delayed Mode QA/QC Best Practice Manual Version 3.1 Integrated Marine Observing
1273 System, doi:10.26198/5c997b5fdc9bd, 2023.

1274 Wood, J. E., Schaeffer, A., Roughan, M., & Tate, P. M.: Seasonal variability in the continental shelf waters off
1275 southeastern Australia: Fact or fiction?. *Continental Shelf Research*, 112, 92-103, doi:10.1016/j.csr.2015.11.006,
1276 2016.

1277 [Zhang, Y., Du, Y., Feng, M., & Hobday, A. J.: Vertical structures of marine heatwaves. *Nature Communications*,
1278 14\(1\), 6483, 2023.](#)

1279 [Zhao, Z., Holbrook, N. J. & Oliver, E. C. J.: An eddy pathway to marine heatwave predictability off eastern Tasmania.
1280 *Front. Clim.* 4: 907828, doi: 10.3389/fclim.2022.907828, 2022.](#)

1281

255

256

257